UNIVERSIDADE D
COIMBRA

DIPTO CHAKRABARTI

Investigation of Mechanical and Tribological Performance of 3D-Printed PLA Composites for Biomedical Applications Reinforced by Carbonaceous and Hydroxyapatite fillers.

VOLUME 1

Dissertation under the Joint European Master's degree in Surface Tribology and Interfaces guided by Prof. Dr. Bruno Trindade presented to the Department of Mechanical Engineering of the Faculty of Science and Technology of the University of Coimbra.

July 2023

FACULDADE DE CIÊNCIAS E TECNOLOGIA
UNIVERSIDADE D COIMBRA

Investigation of Mechanical and Tribological Performance of 3D-Printed PLA Composites for Biomedical Applications Reinforced by Carbonaceous and Hydroxyapatite fillers.

Submitted in Partial Fulfilment of the Requirements for the Degree of European Joint European Master in Tribology of Surfaces and Interfaces.

Comportamento mecânico e tribológico de compósitos de PLA reforçados com carbono e hidroxiapatita para aplicações biomédicas, produzidos por impressão 3D.

Author

Dipto Chakrabarti

Advisor[s]

Prof. Dr. Bruno Trindade

Professor at University of Coimbra

Jury

President	**Prof. Dr. Albano Cavaleiro** **Professor at University of Coimbra**
Vowel	**Profª. Drª. Sandra Carvalho** **Professor at University of Coimbra**
Advisor	**Prof. Dr. Bruno Trindade** **Professor at University of Coimbra**

1 2 9 0 UNIVERSIDADE D COIMBRA

tribos Joint European Master in Tribology of Surfaces and Interfaces
Ljubljana • Leeds • Coimbra • Luleå

Coimbra, July 2023

ACKNOWLEDGEMENTS

I am profoundly grateful to my parents, Bina Rani Das and Dipok Chakrabarti, whose unwavering support and sacrifices have been the driving force behind my educational journey. Despite not having the opportunity for higher education themselves, their selflessness, love, and guidance have propelled me forward, shaping the person I am today.

I wish to express my sincere gratitude to my master thesis advisor, Prof. Bruno Trindade, from the University of Coimbra, for his invaluable guidance, unwavering support, and insightful suggestions throughout the entire process of writing this thesis. His expertise and dedication have been instrumental in shaping the outcome of this work, and I am truly grateful for his mentorship.

Furthermore, I would like to extend my heartfelt appreciation to the staff at IPN, namely Carlos Patacas, António Fonseca, Fábio Cerejo, Todor Vuchkov, Nelson Duarte, Sérgio Henrique de Paiva Lourenço, and Telma Ferreira. Their generous contribution of time and effort in performing the characterization of the project samples has significantly enriched the quality and depth of this research. I would also like to express my sincere thanks to the staff at the Mechanical Department of the University of Coimbra, particularly Gonçalo Olivera, Pedro Soares, Ana Micaela Sousa, Diego Carvalho, and Manuel Evaristo. Their assistance in the production and characterization of the samples has been invaluable and greatly contributed to the successful completion of this thesis.

Special gratitude is extended to Professor Dr. Ana Paula Piedade at the University of Coimbra for her invaluable guidance and expertise during the filament fabrication process. Her profound knowledge and insightful advice have greatly enhanced the quality and reliability of the experimental work conducted in this study.

Finally, I would like to express my deepest appreciation to the TRIBOS consortium and the European Commission for their generous financial support, which has made it possible for me to pursue and complete my master's program. Without their funding, the successful completion of this thesis would not have been possible.

Once again, I am sincerely thankful to all the individuals and institutions mentioned above for their contributions, support, and encouragement throughout this research journey.

RESUMO

Este estudo centra-se na otimização da composição química de materiais compósitos à base de poli (ácido láctico) (PLA), reforçados com carbono, nomeadamente fibras curtas de carbono (SCFs) e nanoplaquetas de grafeno (GNPs), em concentrações variáveis (0,5 a 5 % em peso para cada forma de carbono). O desempenho mecânico e tribológico destas amostras, designadas por PSG, foi avaliado. Adicionalmente, a investigação focou-se também na avaliação das propriedades mecânicas e tribológicas de amostras à base de PLA incorporando hidroxiapatita (HA) como reforço, em concentrações de 5 e 10% em peso (amostras designadas por PH). Para fabrico das amostras, foi usada a impressão 3D de fabricação de filamento fundido (FFF). Os resultados deste estudo revelaram uma dispersão bem-sucedida dos reforços dentro dos compósitos. Nas amostras PSG e PH, a presença de SCF e GNP, e HA facilitou a cristalização dos filamentos de PLA, atuando como agentes nucleadores. À medida que as concentrações dos reforços aumentavam, melhorias notáveis foram observadas na dureza, módulo de elasticidade e resistência específica ao desgaste para ambas as amostras de PSG e PH. Especificamente, o PSG-5, consistindo de um reforço de 5% em peso de SCF + 5% em peso de GNP, exibiu um notável aumento de 30% na dureza em comparação ao PLA puro. Da mesma forma, a adição de 10% em peso de HA (PH-10) resultou num aumento de 6% na dureza. O módulo de elasticidade apresentou uma tendência semelhante, verificando-se aumentos máximos de 220% no caso da amostra PSG-5 e de 202% no caso da amostra PH-10. Para além disso, todas as amostras PLA reforçadas exibiram coeficientes de fricção (COF) mais baixos em comparação com o PLA puro. As amostras de PSG apresentaram valores de COF variando de 0,49 a 0,6, enquanto as amostras de PH mantiveram um valor de COF constante de 0,49 para PH-5 e PH-10, superando o COF de PLA (0,57). A amostra PSG-5 apresentou a menor taxa de desgaste específico (4,04 x 10^{-4} mm3/N.m) entre os compósitos PSG, enquanto a amostra PH-10 exibiu a menor taxa de desgaste em 2,75 x 10-4 mm3/N.m entre os compósitos PH. Esses valores representaram uma redução de desgaste de, respetivamente, 5 e 1,8 vezes em relação ao PLA. Em conclusão, este estudo demonstrou que a incorporação de SCF e GNP, e de HA, na matriz de PLA, melhora significativamente as suas propriedades mecânicas e tribológicas e destacou o potencial desses compósitos para aplicação numa gama ampla de aplicações que exijam a utilização de polímeros com resistência mecânica e resistência ao desgaste melhoradas.

ABSTRACT

This study focuses on optimizing the composition of Poly (lactic acid) (PLA)-based composite materials by reinforcing them with carbonaceous fillers, namely short carbon fibers (SCFs) and graphene nanoplatelets (GNPs), at varying concentrations (ranging from 0.5 to 5 wt.% for each filler). These composite samples, referred to as PSG samples, were thoroughly examined to assess their mechanical and tribological performance. Additionally, the investigation explored the mechanical and tribological properties of PLA-based materials incorporating hydroxyapatite (HA) at concentrations of 5 and 10 wt.%, known as PH samples. To create these samples, fused filament fabrication (FFF) 3D printing was employed. The findings of this study revealed successful dispersion of the fillers within the composites. In the PSG samples, the presence of SCF and GNP facilitated the crystallization of PLA filaments, while in the PH samples, HA acted as a nucleating agent, demonstrating a similar behavior. As the concentrations of the fillers increased, notable improvements were observed in hardness, elastic modulus, and specific wear resistance for both PSG and PH samples. Specifically, PSG-5, consisting of a 5 wt.% SCF + 5 wt.% GNP reinforcement, exhibited a remarkable 30% increase in hardness compared to pure PLA. Similarly, the addition of 10 wt.% HA (PH-10) resulted in a 6% increase in hardness for the PH samples. The elastic modulus displayed a consistent trend, with PSG samples showing a substantial 220% increase and PH samples demonstrating a notable 202% increase. Moreover, all PSG and PH composite samples exhibited lower coefficients of friction (COF) compared to pure PLA. PSG samples demonstrated COF values ranging from 0.49 to 0.6, while PH samples maintained a constant COF value of 0.49 for both PH-5 and PH-10, surpassing the COF of PLA (0.57). Furthermore, PSG-5 showcased the lowest specific wear rate at 4.04×10^{-4} $mm^3/N.m$ among the PSG composites, while PH-10 exhibited the lowest wear rate at 2.75×10^{-4} $mm^3/N.m$ among the PH composites. These values represented a wear reduction of five times for PSG samples and 1.8 times for PH samples compared to different PLA compositions used in the respective composite material systems. In summary, this study demonstrates that the incorporation of SCF and GNP into the PLA matrix, as well as the addition of bioceramic filler HA, significantly enhance the mechanical and tribological properties of the resulting composite materials. These findings highlight the potential of these composites for a wide range of applications that require exceptional mechanical strength and wear resistance.

TABLE of Contents

LIST of FIGURES

LIST of TABLES

LIST of ABBREVIATIONS

Abbreviation	Definition
AM	Additive manufacturing
ABS	Acrylonitrile Butadiene Styrene
BO	Bentonite
CAD	Computer-aided design
CAGR	Compound Annual Growth Rate
CCF	Continuous Carbon Fiber
CF	Carbon Fiber
CNT	Carbon Nanotube
CT	Computer tomography
DSC	Differential scanning calorimetry
EDS	Energy-dispersive X-ray spectroscopy
FFF	Fused filament fabrication
GF	Glass Fiber
GNP	Graphene Nanoplatelet
HA	Hydroxyapatite
LOM	Laminated Object Manufacturing
MWCNT	Multiwalled Carbon Nanotube
NDI	Non-Destructive Inspection
nHAp	Nano-Hydroxyapatite
PEEK	Poly-ether-ether-ketone
PET	Polyethylene Terephthalate
PLA	Polylactic Acid
PLGA	Poly-lactic-co-glycolic acid)
PMC	Polymer Matrix Composite
PTFE	Poly Tetrafluoro Ethylene
SCF	Short Carbon Fiber
SEM	Scanning electron microscopy
UHMPWE	Ultra-High Molecular Weight Polyethylene
XRD	X-ray diffraction

1. INTRODUCTION

Additive manufacturing (AM), also known as 3D printing, is a process of creating three-dimensional objects by adding materials layer upon layer to form the desired shape [1]. This innovative technology has transcended its initial use in prototyping and is now capable of producing robust and safe products for commercial sale in significant quantities. The process uses computer-aided design (CAD) and converts the design into a unique file format, and finally, it is then used by the 3D printer to construct the product layer by layer [2]. The field of applications of 3D printing is vast and includes industries such as medical, aerospace, automotive, art, and manufacturing, where it is used to create prototypes, customized parts, and even entire vehicles, among other applications [3-5]. Especially if it can be successfully put into mass production, the technology has the potential to revolutionize the manufacturing, logistics, and management of inventories industries [6]. In recent years, the rising demand for functional and personalized biomedical devices and implants has prompted the investigation of innovative materials and production techniques. AM, notably 3D printing, has arisen as a formidable tool in biomedical engineering, enabling the production of intricate structures with accuracy [5, 7-9]. According to market projections, the global biomedical 3D printing market was valued at around $1.45 billion in 2021. This market is anticipated to witness substantial growth, reaching an estimated value of approximately $6.21 billion by the year 2030. The projected compound annual growth rate (CAGR) for the period between 2023 and 2032 is expected to exceed 22.5% [10-12]. These figures exemplify the rapid expansion and immense potential of 3D printing in revolutionizing healthcare and biomedical applications.

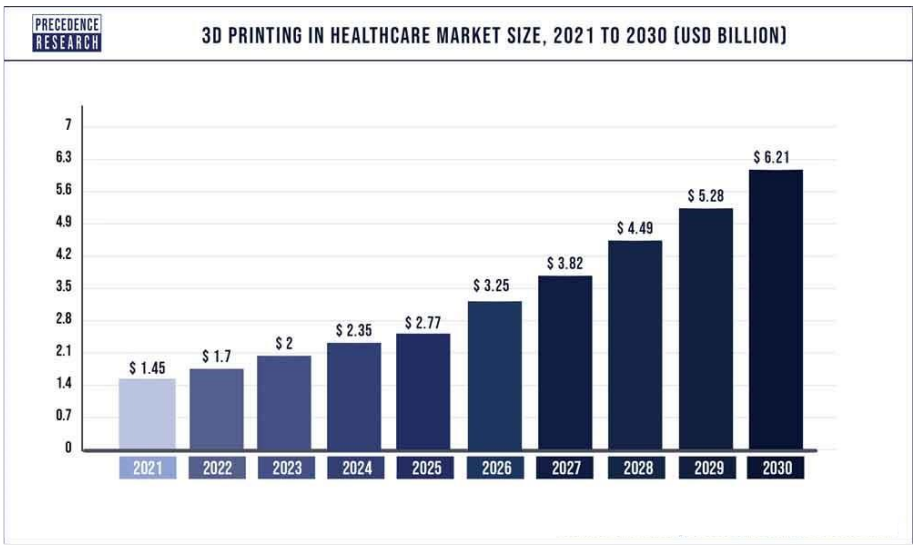

Figure 1. 3D Printing in healthcare market size 2022 to 2030 [12]

The healthcare industry is undergoing a transformative shift with the widespread adoption of 3D printing technology. This innovative manufacturing approach has significant implications for medical device manufacturing, tissue engineering, prosthetics, and personalized medicine. With advantages such as time and cost savings, reduced anesthesia exposure, and enhanced surgical planning, the demand for 3D-printed medical devices is rising. Examples include dental restorations, orthopedic implants, and external prosthetics. The integration of 3D printing in healthcare is revolutionizing patient care and driving advancements in the field [10]. The healthcare industry is benefiting from the advancements of 3D printing, which is enhanced by the vast array of materials employed in additive manufacturing. These materials include polymers, metals, ceramics, composites, smart materials, and other variants [7]. Polymers are the most used material in AM, and common plastics such as acrylonitrile butadiene styrene (ABS), PLA, polycarbonate (PC), polyether ether ketone (PEEK), etc. can be used [13]. In addition to these materials, the adaptability of 3D printing also enables the use of uncommon materials like sticker papers, chocolate, and polymer/adhesive sheets for laminated object manufacturing (LOM). However, it is crucial to remember that the chosen material's characteristics significantly impact the final quality of the printed product [14]. The types of multi-materials, including metal-metal, metal-ceramics, metal-polymer, polymer-polymer, and functionally graded multi-materials, are also reviewed in the literature [15].

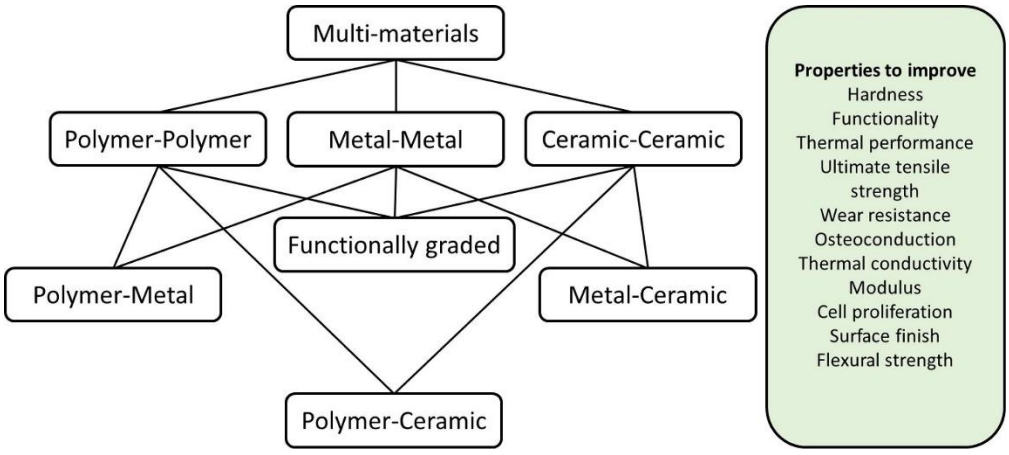

Figure 2. Multi-materials for AM [15].

Among various materials available for 3D printing, PLA has gained significant attention due to its biocompatibility, ease of processing, and desirable mechanical properties. Now with PLA, it is possible to come up with a patient-specific customized solution of biomedical problems [16,17]. However, PLA materials face certain limitations attributed to their poor toughness, low impact resistance, low hydrophilicity, slower degradation rate, and inadequate cell adhesion [16-18]. To meet the demanding requirements of biomedical applications and harness the full potential of PLA when it comes to tailormade solutions, further improvements in the mechanical and

tribological performance of PLA are necessary. In recent years, the incorporation of fillers has shown promise in enhancing the mechanical and tribological properties of PLA-based composites. Among these, SCF, CNT, glass fibers (GF), and GNPs are promising fillers to overcome the existing limitations of the polymer matrix by creating a composite with better structural and functional properties that none of the constituents alone could achieve [19,20]. PLA is a potential biodegradable polymer used as a matrix in polymer-based composites. PLA-graphene nanocomposite blends are actively employed to produce 3D-printed scaffolds for tissue engineering [21]. Although the biocompatibility of this composite has been demonstrated in previous studies [22,23], its prospective application in load-bearing structures, as well as the resulting performance under varying loading situations, should be investigated further. When polymers are used in tribological applications at great velocity under high loads, they exhibit a low load-carrying capacity and a short running life [24], with considerable financial loss to the industry [25]. There is currently significant interest in applying polymer-based composites for tribological applications [26,27]. Carbon fillers, including carbon nanotubes (CNT), carbon fibers (CF), graphene, and others, can be used to improve the tribological behavior of polymer composites [28]. Because of their excellent thermal, mechanical, and electrical properties, high surface-to-volume ratio, and good dispersion in polymer matrices, SCF and GNP are good candidates for the advancement of structural and functional polymer composites [29,30].

Another filler that recovers the inherent osteogenic incapability of PLA is a bioactive ceramic called HA, which is an organic phase core ingredient for bones (60 wt.%) and tooth enamel (90 wt.%) [31]. HA, with the chemical formula Ca10(PO4)6(OH)2, is a biocompatible and biodegradable material that has shown great promise in bone regeneration [32]. The incorporation of HA into PLA-based scaffolds has been explored in the field of bone tissue engineering to enhance their biological properties and promote bone regeneration. The rich carboxyl and hydroxyl groups of the HA structure provide it with a highly hydrophilic character that facilitates cell adhesion and wound healing and can encourage hemostasis, prompt collagen deposition and fibrosis, regulate inflammation balance, and promote re-epithelialization via the enzymatic reaction of hyaluronidase and chemical interaction [32].

The present study aims to investigate the mechanical and tribological performance of 3D-printed PLA composites reinforced with carbonaceous fillers (SCFs and GNPs) and HA fillers. First, the optimal composition of the PLA-based composite with carbonaceous fillers will be determined through systematic experimental investigation. Mechanical characterization, including tensile strength, flexural strength, and impact resistance, will be conducted to evaluate the performance of the composites. Furthermore, the tribological properties of the PLA-based composites with HA fillers will be assessed through wear tests and friction tests. These evaluations will provide insights into the wear rate, coefficient of friction, and surface morphology of the composites. In vitro biocompatibility tests, including cell viability and proliferation assays, will be carried out to evaluate the cytocompatibility of the composites, ensuring their suitability for biomedical

applications. The findings from this research will contribute to the development of advanced 3D-printed PLA composites with enhanced mechanical strength, wear resistance, and biocompatibility. Such composites have great potential for use in various biomedical applications, including bone tissue engineering, orthopedic implants, and other load-bearing biomedical devices.

2. BACKGROUND

2.1 PLA

2.1.1 Properties and Characteristics of PLA

PLA is a bio-based and biodegradable polymer that has garnered considerable interest owing to its distinctive characteristics and diverse array of potential uses. Comprehending the properties and characteristics of PLA is imperative for investigating its potential as a matrix material in composite systems. This section presents a comprehensive overview of the fundamental properties and distinctive characteristics of PLA.

1. Mechanical Properties: PLA demonstrates a synergistic interplay between its elastic modulus and fracture toughness, rendering it a viable candidate for diverse mechanical loading scenarios. The tensile strength of the material generally falls within the range of 50 to 70 MPa, while Young's modulus varies between 2 to 5 GPa, strain at fracture is around 4-10% based on the grade and processing parameters [17,33,34].

2. Thermal Properties: Semi-crystalline PLA exhibits a modest glass transition temperature (Tg) of approximately 55-58°C, which governs its thermal stability and processability. Upon surpassing the glass transition temperature (Tg), PLA undergoes a transition from a vitreous phase to a viscoelastic phase, thereby enabling malleability and plasticity [35]. PLA demonstrates a melting temperature (Tm) that generally falls within the range of 130 to 230 °C. The thermal characteristics of PLA render it appropriate for diverse processing methodologies, including but not limited to extrusion, injection molding, and additive manufacturing via 3D printing [36].

3. Biodegradability: One of the principal benefits of PLA is its inherent biodegradability. Polylactic acid (PLA) is a biopolymer from renewable resources, including corn starch or sugarcane [37]. It degrades, undergoing first hydrolytic and latter enzymatic degradation in industrial composting facilities and natural environments [38]. The eco-friendliness of PLA as a substitute for petroleum-based plastics leads to a decrease in environmental impact and advancement in sustainability.

4. Transparency and Appearance: PLA is renowned for its exceptional transparency, akin to that of traditional plastics used in food packaging applications such as polyethylene terephthalate (PET) and polystyrene (PS). The surface of the material exhibits a lustrous quality and can be readily pigmented or manipulated to attain diverse optical outcomes [39]. The inherent aesthetic properties of PLA render it a viable option for deployment in scenarios necessitating transparency or visual allure, such as the packaging of comestibles and consumer goods.

5. Processability: PLA exhibits favorable processability characteristics, facilitating diverse shaping techniques, including but not limited to injection moulding, extrusion, blow moulding, and film casting [36]. Compared to other biopolymers, PLA has better thermal processability, reduced energy consumption, and improved manufacturing efficiency [17].
6. Barrier Properties: PLA demonstrates moderate barrier characteristics against gases, including oxygen and carbon-dioxide, aroma molecules, and water vapor, thereby rendering it appropriate for deployment in packaging-related domains. Nevertheless, its barrier characteristics exhibit inferiority in comparison to other petrochemical-derived polymers, such as PET [40]. To augment the barrier properties PLA, it is possible to utilize multi-layer or nanostructured coatings [41].

2.1.2 Limitations and Disadvantages of Neat PLA

Although PLA presents various benefits, it also exhibits specific constraints and drawbacks that require careful consideration. Comprehending these constraints is pivotal in formulating tactics to surmount them and enhance the efficacy of materials based on PLA. This section presents a comprehensive overview of the principal constraints and drawbacks linked to neat PLA.
1. Brittleness: One of the principal constraints of neat PLA is its intrinsic fragility. It demonstrates a relatively low impact strength and tends to display brittle fracture behavior under specific conditions with less than 10% elongation at break [17]. This constraint restricts its utilization in scenarios that necessitate elevated tenacity and endurance against impact or dynamic loading.
2. Processing Temperature: PLA exhibits a comparatively low thermal resistance and possesses a processing temperature range that is more limited in comparison to certain other polymers. Generally, it exhibits a glass transition temperature (Tg) ranging from 55-65 °C, which may pose challenges to its processability in specific applications such as injection molding or blow molding, electrical applications, thermoforming, etc. [42]. Elevated processing temperatures have the potential to induce thermal degradation, whereas reduced temperatures may give rise to suboptimal melt flow and processing challenges.
3. Slow degradation rate: The degradation rate of PLA is characterized by its slow hydrolysis of ester groups. The degradation rate is subject to the influence of various factors, including but not limited to PLA crystallinity, molecular weight, structure, diffusion of water level, and stereoisomeric information [43]. Decelerated degradation kinetics can lead to a prolonged lifespan of several years, which may not be optimal for scenarios that mandate regulated degradation, such as specific biomedical applications.
4. Hydrophobicity: PLA displays a degree of hydrophobicity, indicating its tendency to repel water. This phenomenon may result in decreased cellular and tissue affinity and, in certain instances, elicit an inflammatory reaction upon exposure to biological fluids [44]. Enhancing the hydrophilicity of PLA surfaces is crucial in augmenting its cellular interaction, particularly in biomedical applications.

5. Chemical Inertness: The absence of reactive groups in PLA makes it chemically inert. This constrains the capacity to introduce functional groups in the sidechain or alter the surface and bulk properties of the material via conventional chemical techniques [36].

2.2 Enhancing the Performance of PLA Composites

2.2.1 Importance of Reinforcing Agents in Improving the Mechanical Properties of PLA

The mechanical characteristics of PLA composites are significantly improved by reinforcing agents. The PLA matrix can be modified by adding various agents to change critical mechanical properties such as strength, stiffness, toughness, and wear resistance [45]. There are various advantages of adding reinforcing agents to the PLA matrix. First and foremost, it improves the composite's strength and stiffness, addressing neat PLA's innate brittleness and low tensile modulus [46]. The reinforcing agents serve as load-bearing elements in the composite structure, efficiently transferring stress and enhancing overall mechanical performance [47-49]. Second, the toughness and impact resistance of PLA composites is improved by the reinforcing agents. Neat PLA has limited use in situations requiring great energy absorption and impact resistance due to its comparatively poor fracture toughness and impact strength [50,51]. Moreover, the incorporation of reinforcing agents has the potential to improve the tribological characteristics and wear resistance of PLA composites [52].

The efficacy of reinforcement agents in enhancing the mechanical characteristics of PLA composites can be attributed to multiple mechanisms. The load transfer mechanism encompasses the transmission of externally applied stress from the matrix to the reinforcing agent, thereby facilitating the uniform distribution of the load and impeding the propagation of cracks [53]. The interfacial bonding mechanism between the reinforcing agent and the PLA matrix is of paramount importance in guaranteeing efficient stress transfer and load-bearing capacity. Moreover, the dispersion and alignment of the reinforcing agents within the matrix exert a substantial impact on the mechanical properties of the composite [54].

2.2.2 Reinforcement Approaches for PLA Composites

To harness the potential of PLA while balancing its limitations, researchers have directed their attention toward reinforcing PLA with diverse substances and transforming it into different PLA-based composite materials. Since the matrix is based on PLA which is a polymer these composites are also termed as polymer matrix composite (PMC). PMCs refer to composite materials that employ a polymer resin as the matrix material. PMCs possess favorable characteristics such as

low weight, high stiffness, and robustness, rendering them highly suitable for deployment in the aerospace and automotive sectors. The matrix within PMC is of paramount importance in facilitating fiber bonding and load transfer [55]. The reinforcement material may manifest in the configuration of fibers, particles, or nanofillers. Blending reinforcement agents into PLA can substantially enhance its mechanical characteristics, including tensile strength, flexural strength, and impact strength. Numerous investigations have been carried out to examine the impact of fiber reinforcement on the mechanical characteristics of PLA. Incorporating fibers into the composite material significantly enhances its mechanical properties, particularly in terms of high tensile strength and stiffness [56]. The optimized alignment of fibrous structures amplifies the load-bearing efficacy and impedes the propagation of cracks, thereby culminating in heightened toughness. Numerous studies have shown that adding natural fibers, glass fibers, short carbon fibers, and ceramic fillers can improve the mechanical properties of PLA and allow it to be used in the intended applications [57-60]. Additionally, the researchers examined and found that CNTs, GNPs), nano-hydroxyapatite (nHAp), and nano clay were successful in imparting the desired qualities to PLA, improving both its mechanical and barrier capabilities [61-63]. In PLA composites used for biomedical applications, bioceramic elements, including HA, calcium phosphate, and bioactive glass, are frequently included, strengthening the composite while encouraging bone repair [30]. According to studies, adding HA improves the mechanical properties of ceramic scaffolds, and adding bioactive and biocompatible fillers to ceramic-polymer composites improves cell adhesion. It makes developing new bone tissue easier after implantation [64-66].

2.3 Overview of the Growing Interest in PLA-Based Composites

The recent surge in interest in composites derived from PLA can be attributed to several factors. Firstly, there is an ever-growing demand for sustainable materials in various industries, such as packaging, automotive, aerospace, and biomedical sectors. This need has encouraged researchers to explore environmentally friendly alternatives to traditional petroleum-based polymers. Secondly, the ability to customize the characteristics of PLA by incorporating reinforcement materials has sparked extensive scholarly investigation. Researchers aim to enhance the mechanical functionality, thermal stability, flame retardancy, and other functional properties of PLA by integrating reinforcing agents into its matrices [67]. The versatility of PLA composites allows for tailoring them to specific applications, thereby expanding their potential use in diverse industries. To enhance the qualities of PLA composites, researchers have examined various types of reinforcing agents. The choice of reinforcing material depends on the desired characteristics of the composite and the specific application at hand. Different processing methods, such as melt blending, solution casting, and 3D printing, have been explored to incorporate reinforcing agents

into the PLA matrix [68]. The growing interest in PLA-based composites stems from the opportunity to combine the desirable properties of PLA with the improved mechanical performance offered by the reinforcing agents. Researchers can optimize the formulation and processing parameters of the composite by understanding the interactions between the PLA matrix and the reinforcing materials to achieve the desired properties.

Carbonaceous fillers including, CNT, CF, graphene, and others, are used to improve the mechanical and tribological behavior of polymer composites [28]. Because of their excellent thermal, mechanical, and electrical properties, high surface-to-volume ratio, and good dispersion in polymer matrices, SCF and GNP are good candidates for the advancement of structural and functional polymer composites [29,30]. Ferreira *et al.*[69] have shown in their study (Figure 3) that incorporating short carbon fiber can enhance the mechanical properties of printed PLA and positively affects the tensile and shear modulus in various printing directions.

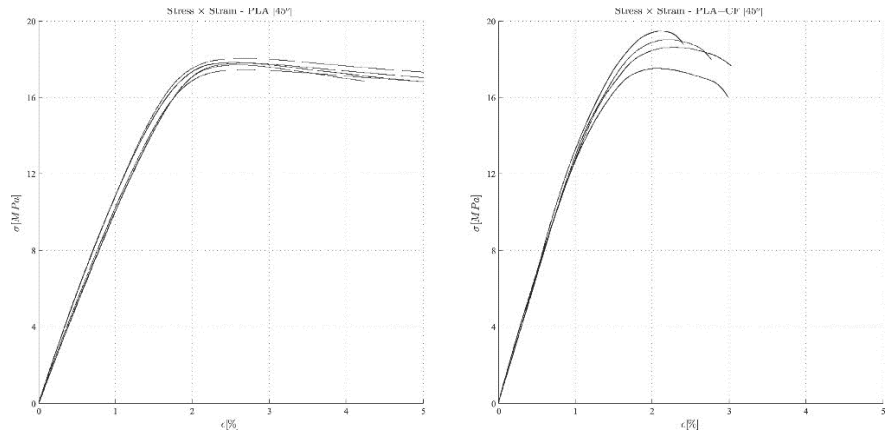

Figure 3. Effect of SCF reinforcement into PLA at ±45^0 printing orientation [69].

Another study by Rarani *et al.*[70] have shown from their experiments that, upon incorporating continuous carbon fiber (CCF) into PLA, the ultimate tensile strength and tensile modulus of elasticity during tensile tests and bending modulus and bending strength increases by fairly a large margin indicating an overall improvement in the mechanical behavior of the material than pure PLA. Figure 4a shows the tensile stress-strain curve of pure PLA and CCF/PLA composite, and figure 4b illustrates load-displacement curves during three-point bending tests of both raw and composite PLA material.

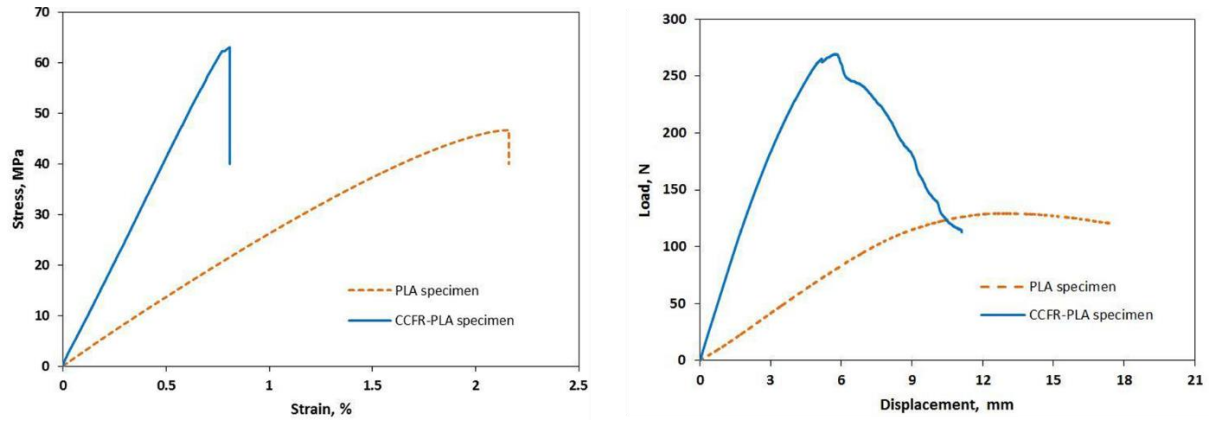

Figure 4. Effect of CCF reinforcement into PLA (a) tensile stress-strain curve of pure PLA and CCF-PLA specimens (b) load-displacement curves of pure PLA and CCF-PLA under three-point bending test [70].

Similarly, introducing graphene nanoplatelets into PLA can affect its mechanical properties depending on factors such as raster direction and nanoplatelet size. One study conducted by Vidakis *et al.*[71] have found that graphene-reinforced PLA doesn't improve the mechanical properties of the polymer matrix (Figure 5). However, this effort isn't completely lost since it imparts electronic properties into the composite, enhancing the functional properties of the material.

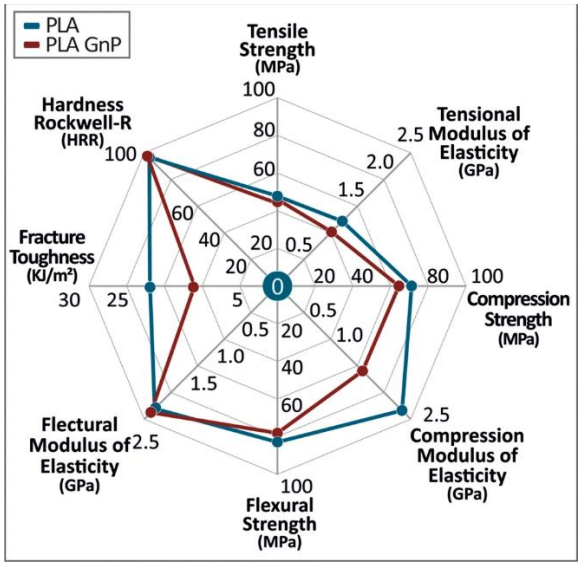

Figure 5. Comparison of the overall mechanical response of FDM-printed PLA polymer versus PLA/GNP composite [71].

However, another study conducted by Gao *et al.*[72] have shown (Figure 6) that improvement of the mechanical properties of the PLA matrix is possible, but it depends on the size of the filler. From their study, it was observed that GNP in 5 wt.% content with a diameter of 15 μm which was considered large, or GNP-L and GNP-s with a diameter of 1 μm which was considered as

smaller filler size, have differences in their mechanical properties. Larger GNP platelet of 15 micrometers at 5 wt.% shown the best mechanical behavior compared to non-reinforced polymer.

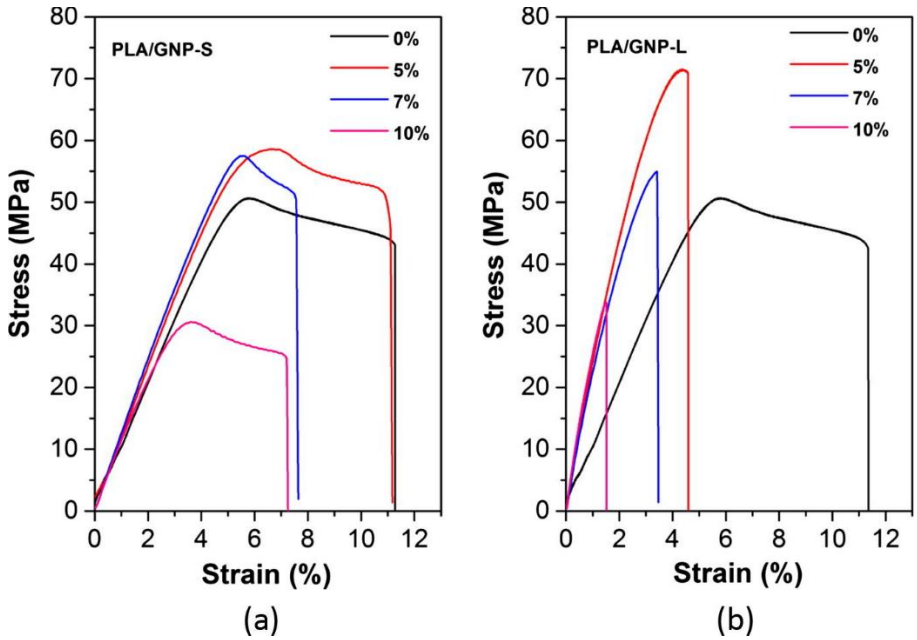

Figure 6. Stress–strain curves of nanocomposite films for; (a) PLA/GNP-S and (b) PLA/GNP-L, showing the highest mechanical reinforcement for 5 wt.% GNP-L based nanocomposites and fully preserved ductility for systems based on 5 wt.% GNP-S [72].

Multiwalled carbon nanotubes (MWCNT) have also been studied as reinforcements for PLA, with concentrations exceeding 1 wt.% found to significantly enhance its mechanical properties [73, 74]. In addition, the incorporation of multiple carbon nanofillers has been investigated due to their impact on the mechanical properties of PLA nanocomposites, with Batakliev *et al.*[75] showing that (Figure 7) combining GNP and MWCNT nanocomposites with better mechanical properties could be obtained.

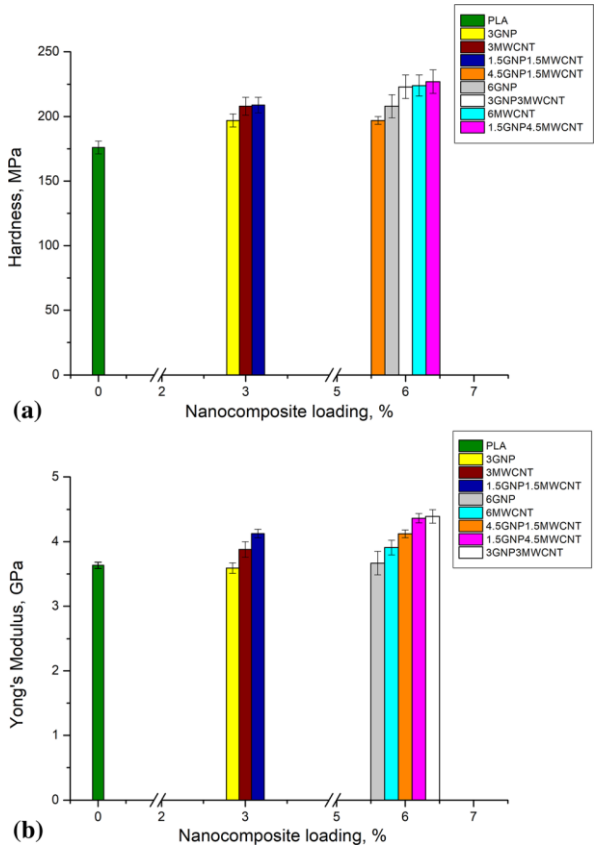

Figure 7. Hardness (a) and Youngs modulus (b) of GNP/MWCNT/PLA nanocomposites with overall 3 and 6 wt.% carbon loading [75].

Basheer *et al.*[76] demonstrated (Figure 8) that adding both SCF and graphene to PLA doubles the mechanical strength of the matrix. Their study shows that, both reinforcement and raster orientation influence the mechanical properties by a significant margin.

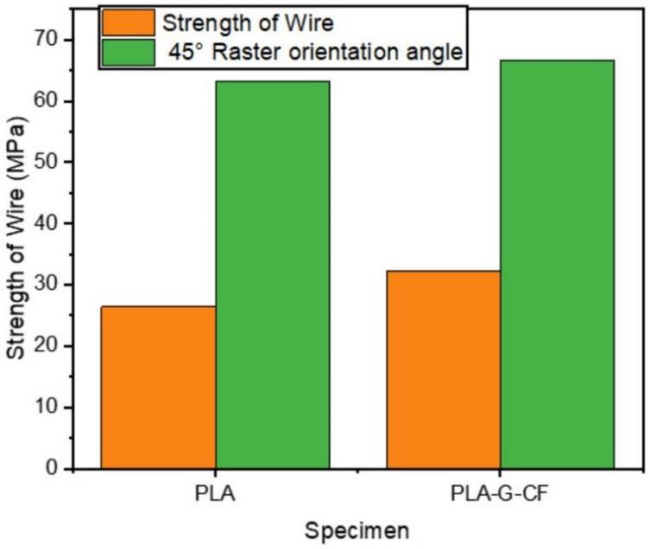

Figure 8. Strength of raw polylactic acid and hybrid polylactic acid (PLA−G−CF) material under tensile load [76].

With respect to the tribological properties, there are few studies available on the effect of adding carbonaceous fillers to PLA. Batakliev *et al.*[77] studied the influence of MWCNTs and GNPs on the tribological behavior of PLA using scratch and wear experiments and claimed that the scratch resistance of the 12 wt.% GNP/PLA nanocomposite was twice as high as neat PLA. Bustillos *et al.*[78] studied the influence of graphene on PLA and showed that PLA-graphene composites presented a significant improvement in creep and wear resistance. Suresha *et al.*[79] have demonstrated that adding 20 wt.% short carbon fibers to PLA resulted in composites with improved wear resistance (70 % decrease in specific wear rate). From Figure 9 it is observed that with the increase of load (10 to 20 N), the increment in mean specific wear rate for SCF-reinforced PLA is less compared to the pure ones.

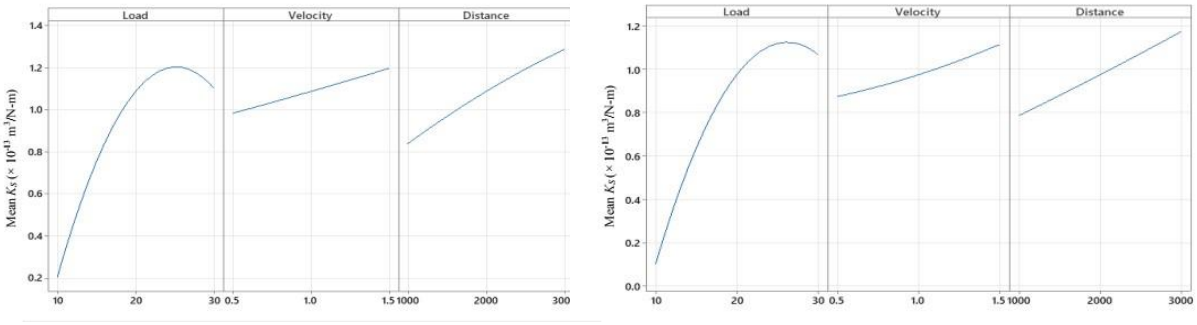

Figure 9. Effect of control factors on KS (a) PLA and (b) PLA reinforced with SCF [79].

In a recent work on PLA-based biocomposites reinforced with SCF, GNP, and SCF + GNP [52] produced by casting, it was shown that the joint addition of these two fillers (volume ratio between the PLA and the fillers of 1:0.02) had a beneficial effect on the hardness and specific wear

rate of PLA. The use of bioceramic materials, including HA, calcium phosphate, and bioactive glass, is prevalent in PLA composites for biomedical purposes. The materials used have a dual function of strengthening the composite and promoting bioactivity, which aids in the regeneration of bone and osseointegration. The use of ceramic nano biomaterials, specifically those based on calcium phosphate, has been the subject of numerous studies in the fields of orthopedics and dentistry [61]. These materials have been investigated for their potential applications in a wide range of scenarios. One common type of material used in biomedical applications is bioceramics [80]. Incorporating synthetic biopolymers like HA as coatings on poly (lactic-co-glycolic acid) (PLGA) surfaces can enhance the mechanical properties of ceramic scaffolds. Additionally, ceramic-polymer composites are utilized in the biological field [64,66]. These composites present a workable option regarding mechanical strength, biological usefulness, and biocompatibility. The addition of bioactive and biocompatible fillers enhances the ability of bone cells to adhere, proliferate, and differentiate. This ultimately leads to the formation of new bone tissue when implanted [65]. Concerning tribological properties, several studies have investigated the impact of HA incorporation in polymer blends. The composite's rigid contact points of HA particles are more unyielding against the counter body than the polymer matrix's rigid contact points. Studies have shown that adding HA to polymer matrices like ultra-high-molecular-weight polyethylene (UHMWPE) improves tribological characteristics and wear resistance. For instance, Macuvele *et al.*[81] investigated the application of organophilic bentonite (BO) to improve the interface between UHMWPE and HA, enhancing the composite's mechanical and wear properties. The combined mechanical, tribological, and biological advantages led them to conclude that the composite might be employed in bone tissue engineering [81]. Figure 10 clearly shows that the incorporation of HA into UHMPWE matrix improves the wear and friction behavior of the polymer.

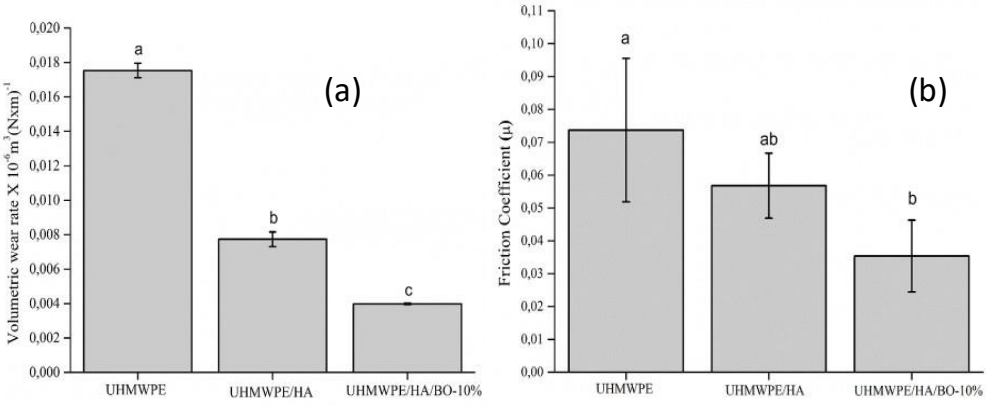

Figure 10. Effect on UHMPWE (a) Volumetric wear rate and (b) Friction coefficient [81].

Experiments with various HA composites (including 7 wt.% nHAp) and UHMWPE demonstrated decreased friction coefficients and wear rates [82]. When 50wt.% nHAP was incorporated into UHMPWE, Mirsalehi *et al.* significantly reduced friction and wear [83]. In a related study, Maksimkin *et al.* found an improved wear resistance of UHMWPE when combined with HA [84]. Kang *et al.*[85] have shown that (Figure 11) nHAp gives better performance both mechanically and tribologically compared to HA when incorporated into UHMPWE. However, to the best of the author's knowledge, no such tribological investigations have yet been conducted on the PLA/HA composite material system.

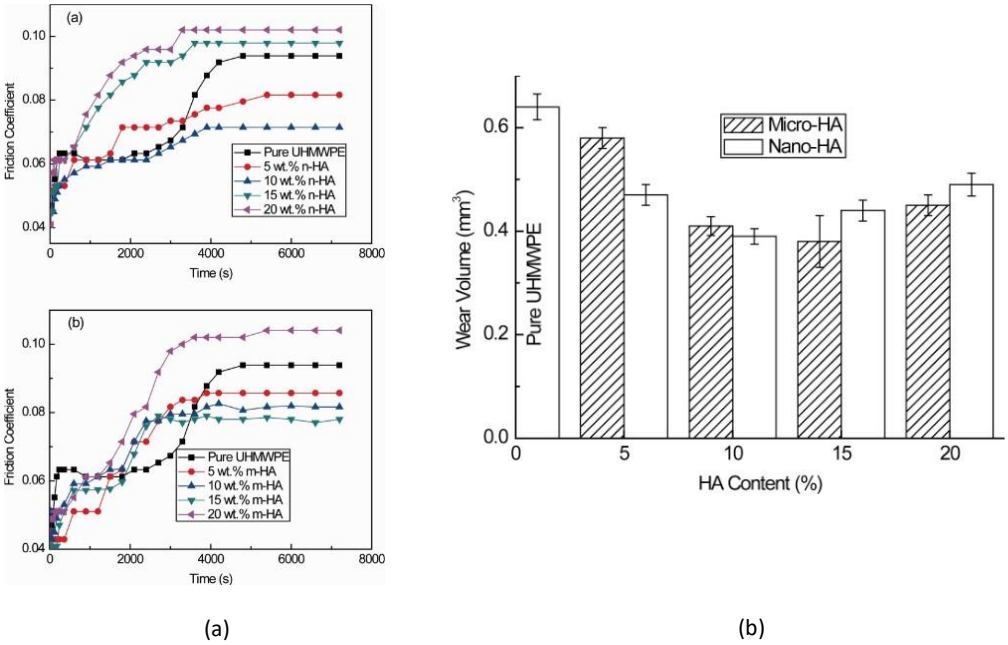

Figure 11. Effect on UHMPWE (a) Friction coefficient and (b) Volumetric wear rate [85].

2.4 Wide Range of Applications for PLA-Based Materials

PLA and its composite materials provide a versatile platform for various applications across multiple industries. The distinctive amalgamation of characteristics, including biodegradability and processability, renders PLA a compelling option for sustainable substitutes to traditional petroleum-derived polymers. This section presents a comprehensive survey of the multifarious applications wherein materials based on PLA have been utilized.

1. Packaging: PLA has garnered substantial attention in packaging due to its biodegradable nature, transparent appearance, and commendable mechanical characteristics. It finds utility in various applications, including but not limited to food containers, blister packs, films, and trays [36]. Using PLA-based packaging offers an environmentally sustainable alternative, thereby mitigating the ecological ramifications of disposable plastics.

2. Biomedical and Healthcare: The biocompatibility and biodegradability of PLA render it appropriate for diverse biomedical and healthcare applications. The utilization of this material is observed in medical devices, drug delivery systems, tissue engineering scaffolds, and sutures [86-92]. PLA-based materials exhibit regulated release characteristics and controlled degradation rates, thereby enabling their application in the fields of regenerative medicine and implantable devices [40,93,94].

3. Textiles and Apparel: PLA fibers have been formulated as an eco-friendly substitute for synthetic fibers derived from petroleum, such as nylon and polyester. These fibers demonstrate favorable mechanical strength, thermal endurance, and moisture sorption characteristics [95]. They are utilized in the domains of textiles, apparel, nonwoven fabrics, and home textiles, thereby making a significant contribution towards the promotion of sustainable and environmentally friendly fashion.

4. Agriculture and Horticulture: PLA-based materials have been used in agriculture and horticulture. Their films are utilized together with plasticizers for mulching purposes, thereby facilitating weed suppression, moisture preservation, and regulation of soil temperature [96]. Plant pots and trays based on PLA offer a biodegradable substitute for traditional plastic receptacles, mitigating the accumulation of refuse and ecological contamination.

5. 3D Printing and Prototyping: The processability and compatibility of PLA with additive manufacturing techniques, including 3D printing, have rendered it a prevalent material in prototyping and small-scale production. PLA filaments are extensively utilized in desktop 3D printers owing to their facile printability, minimal warping, and broad accessibility [97]. PLA has emerged as a promising material for 3D printing applications, especially in the domain of biomedical devices and a wide range of manufacturing and architectural applications [98]. The utilization of PLA 3D printing has brought about a significant transformation in the creation of personalized medical devices that are based on patient-specific anatomical information and computer-aided design. This technology holds immense promise in the fields of tissue engineering, diagnostic platforms, and drug delivery systems [99].

6. Consumer Goods: PLA-based materials are utilized in a variety of consumer products, such as single-use utensils, food containers, disposable drinkware, and playthings. The utilization of polylactic acid's biodegradability, aesthetic appeal, and food contact suitability confer advantageous attributes to these applications [36].

3. RESEARCH GAP AND OBJECTIVE

In a previous investigation conducted by Anzum Al Abir [52], the Tribos+ master thesis studied the mechanical and tribological behavior of PLA reinforced with Sn-Zn-Bi, SCF, and graphene. The study yielded promising results regarding the PSG composition, thereby opening avenues for exploring the optimal composition of this composite material system. By conducting further experiments and meticulously analyzing the results, it is possible to establish a scientifically rigorous correlation between the reinforcement content and the beneficial characteristics of the PLA/SCF/PSG composite.

Another intriguing application of PLA lies in the field of biomedical scaffolding. Scaffolds play a crucial role in tissue engineering, facilitating the regeneration process at fractured bone sites. In bone tissue regeneration, it is common practice to employ a scaffold positioned between the site of the bone fracture and the subsequent injection of stem cells. This scaffold aids in the regeneration of bone tissue. PLA has gained popularity in biomedical applications due to its bioresorbability, biocompatibility, and satisfactory mechanical properties, which allow for customized orthopedic solutions tailored to individual patients. However, it is important to note that PLA has limitations in terms of bioactivity. For example, it lacks the ability to promote cell adhesion and the osteogenic capability required for the differentiation of stem cells into osteoblasts, responsible for bone tissue formation. Researchers have explored the incorporation of HA into PLA scaffolds, testing them in laboratory settings (in vitro) and living organisms (in vivo). The results demonstrated favorable mechanical and biological responses in the PLA/HA composite. However, the tribological analysis of this material system has been overlooked. Microscopic movement at the bone site can lead to scaffold degradation, triggering inflammatory reactions and other undesirable cellular responses. Therefore, investigating the tribological degradation of PLA/HA composites with incorporated HA fillers is crucial.

The primary objectives of this study are to identify the optimum composition for producing a self-lubricating reinforced PLA composite using carbonaceous fillers (SCF and GNP) and to investigate the mechanical and tribological properties of a bioceramic (HA) incorporated PLA composite.

4. EXPERIMENTAL DETAILS

4.1 Materials and Methods

This study focuses on the development and investigation of two distinct material systems: PLA reinforced with GNP and SCF composites, referred to as PSG, and PLA filled with HA composites, referred to as PH samples. The PSG samples were examined in their original state after being printed from the filament developed earlier. In contrast, the PH samples underwent a four-stage process before printing the composite material sample. These stages included mixing and melting, granulation, filament extrusion, and, finally, 3D printing. The workflow of this process is depicted in Figure 13.

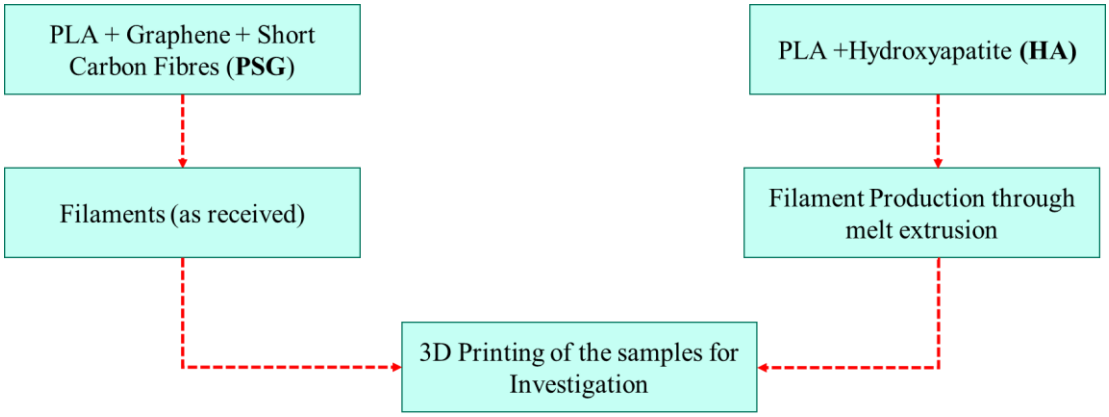

Figure 12. Workflow of PLA-based PSG and PH composite material investigation.

The previous study [52] provided a description of the materials utilized for PSG filaments. The PLA granules (average diameter of 4.85 mm and density of 1.25 g/cm3) were supplied by Goodfellow. SCF (density of 1.8 g/cm3) was provided by Sigrafil with an average filament length of 80 μm and diameter of 7 μm. GNP (purity 99.9% and density of 2 g/cm3), with an average thickness of 5 nm and length of 30 μm, was supplied by Nanografi. The PLA utilized for the second set of composite materials (PH-5 and PH-10) was provided by Sigma-Aldrich. The PLA had an average diameter of 4.85 mm and a density of 1.25 g/cm3. The same company supplied HA (with a density of 1.8 g/cm3) that had an average diameter of ≤ 10μm.

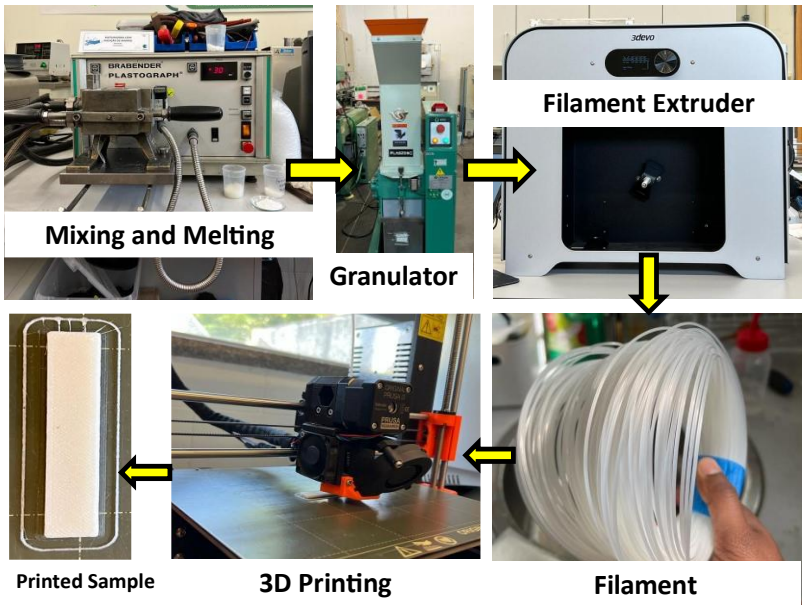

Figure 13. 3D printed samples' manufacturing process: mixing and melting of the PLA granules with reinforcements, granulation of the mixtures, extrusion of the filaments, and 3D printing. The filaments and the 3D samples produced are also shown.

During the production of PSG filaments, the torque was continuously measured as a function of time while mixing PLA with SCF and GNP. After 30 minutes of melting at 190°C and mixing inside the barbender Plastograph homogeneous PSG filaments were obtained [100]. To produce PH filaments, the constituent materials were mixed and melted at 210°C for the same duration inside the same machine. Later, the mixtures obtained were then granulated in Plaszone equipment. After that, the filaments from PLA filled with HA were extruded by a 3Devo extruder machine, while previously, PSG filaments were produced in Barbender equipment [100]. In both cases, the 3D printed samples were produced by FFF (Prusa i3 MK3 3D printer). The printing parameters are indicated in Table 1.

Table 1. 3D printing parameters.

Parameter name	**Value**
Printed sample dimensions (mm)	60x10x3
Extruder Temperature (°C)	215
Bed	Painter's tape
Bed Temperature (°C)	60
Cooling (Fan speed)	100%
Layer Thickness (mm)	0.2
Raster Angle (°)	-45/+45
Infill Density (%)	100%
Nozzle diameter (mm)	0.8

Table 2. Name and chemical composition of the samples produced in this work.

Sample name	PLA (wt.%)	SCF (wt.%)	GNP (wt.%)	HA (wt.%)
PSG-0.5	99	0.5	0.5	-
PSG-1	98	1	1	-
PSG-2	96	2	2	-
PSG-5	90	5	5	-
PH-5	95	-	-	5
PH-10	90	-	-	10

4.2 Characterization Techniques

4.2.1 Morphological and Chemical Characterization

4.2.1.1 Scanning Electron Microscopy (SEM) / Electron Dispersive Spectrometry (EDS)

SEM-EDS is a widely employed method for analyzing and evaluating various materials. This technology has been extensively employed across diverse disciplines such as geology, metallurgy, microelectronics, ceramics, coatings, cement, and soft materials. The fundamental principle underlying EDS involves the utilization of an electron beam to induce the emission of X-rays from a specimen, thereby enabling the acquisition of chemical information about the sample. Except for hydrogen and helium, all elements in the periodic table can be qualitatively analyzed using EDS, while SEM offers topographic information about the sample [101]. Before and after tribological experiments, the morphology of the printed samples was examined using SEM (Hitachi-SU3800) equipment. The chemical composition was determined using energy-dispersive X-ray spectroscopy (EDS) with the X-MaxN, Oxford Instruments, Abingdon, UK. (Figure 14)

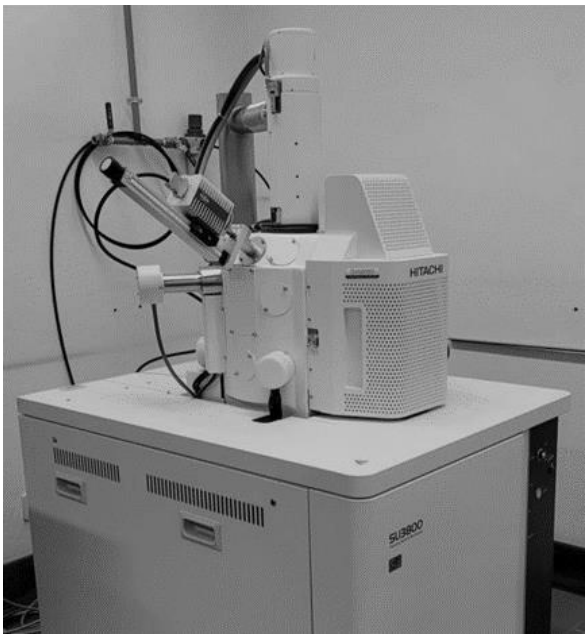

Figure 14. SEM (Hitachi-SU3800) used in this work.

4.2.1.2 Tomography

Computer tomography (CT) is an emerging non-destructive inspection (NDI) method that holds significant relevance in industrial settings. It is particularly valuable when the 3D characteristics of materials are crucial or when monitoring the development of critical features is of interest, be it during the manufacturing process or while in service. CT is a powerful imaging technique that offers both qualitative and quantitative analysis of the structural and compositional characteristics of various materials, including composite materials. It is a widely employed technique within the domain of polymer composites for the purpose of examining the internal structure of said composites. This analysis encompasses the assessment of various aspects, such as the distribution of fibers and voids, as well as the quantification of porosity and density of the composite material. CT is a valuable technique that can be employed for investigating the mechanical characteristics of composites, including their stiffness and strength. Additionally, this technique enables the identification and assessment of defects within composites, such as cracks and delamination. Nevertheless, there are still obstacles to overcome when employing CT for composite materials. These challenges encompass the limited scanning volume in relation to the composite architectures and components, as well as the requirement for image processing to achieve quantitative analysis [102,103]. The tomographic analysis in this study was conducted using SKYSCAN X-ray microtomography (Figure 15).

Figure 15. SKYSCAN X-ray microtomography equipment used in this work.

4.2.1.3 3D Profilometry

3D profilometry is a non-contact surface measurement technique that provides quantitative information about the surface topography of composite materials. The technique involves scanning the surface of the material with a laser or stylus to obtain a 3D map of the surface. The data obtained from the scan can be used to measure the roughness, waviness, and other surface features of the composite material. 3D profilometry is a useful tool for the characterization of composite materials, as it can provide information about the surface morphology of the material, which is important for understanding the mechanical properties of the composite. The technique is also useful for quality control and process optimization in the manufacturing of composite materials [104]. Utilizing an Alicona-InfiniteFocus 3D profilometer (Figure 16), an analysis was conducted on the wear track and scar present on the samples.

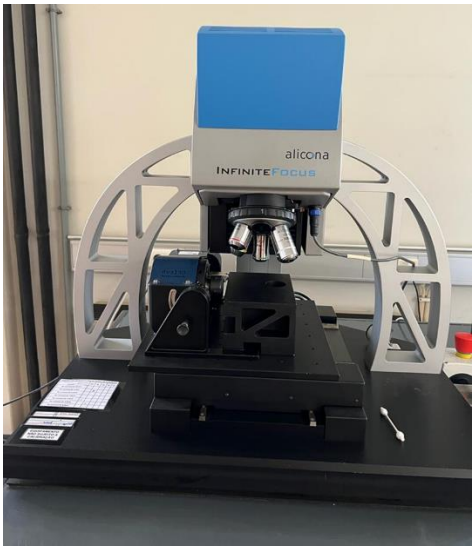

Figure 16. 3D profilometer (Alicona-InfiniteFocus) used in this work.

4.2.2 Structural Characterization

X-ray diffraction (XRD) is a prevalent technique in materials science investigating materials' atomic and molecular structure. The methodology is founded upon X-ray interaction with the crystal lattice of the substance, thereby inducing the X-rays to disperse in diverse orientations. By analyzing scattered X-rays' angular and intensity distribution, researchers can discern the interatomic spacing within the crystal lattice and the atomic type and arrangement. The data can be utilized to determine the substance's crystallographic configuration, chemical makeup, and physical characteristics. XRD is a unique technique for analyzing crystalline substances, including metals, minerals, ceramics, and semiconductors.

Additionally, it can be applied to the investigation of non-crystalline materials, such as amorphous solids and glasses. The non-destructive methodology can investigate materials in diverse forms, such as powders, thin films, and single crystals. It is a potent instrument for materials research. It has a wide range of applications, including the characterization of materials, quality control, and the development of novel materials with tailored properties [105]. The crystalline structure of the raw materials and composites was analyzed via XRD using Co-Ka radiation (1.790300 Å) on a Philips XPert instrument (Figure 17).

Figure 17. Philips XPert XRD equipment used in this work.

4.2.3 Thermal Characterization

Differential scanning calorimetry (DSC) is a thermal analysis technique widely employed to investigate the thermal behavior of materials. It is exact and has gained significant popularity in the scientific community. This methodology enables the quantification of the thermal energy

differential necessary to elevate the temperature of a specimen relative to a reference substance as a temperature-dependent variable. DSC is a commonly employed technique for characterizing polymeric materials. It enables the determination of their thermal behavior and transformations. Through quantifying the thermal energy transfer linked with the specimen, DSC can furnish insights into thermal phenomena encompassing glass transition temperature (Tg), crystallization temperature (Tc), and melting temperature (Tm). DSC is a highly valuable technique for analyzing the thermal stability of various materials, including polymers. It enables the assessment of their thermal properties, such as heat capacity, enthalpy, and thermal conductivity. The methodology can additionally be employed to scrutinize reaction kinetics, phase transitions, and chemical reactions that entail alterations in heat flow [106]. DSC was employed to evaluate the alterations in thermophysical characteristics and crystalline structure of the PLA matrix. The temperature range for all samples was between 25 ^{0}C and 230 ^{0}C. The temperature ramp was set to 10 degrees Celsius per minute, and the carrier gas used was nitrogen at a flow rate of 40 milliliters per minute.

The assessment of the crystallinity degree of the composite powders after compaction was conducted utilizing the equation [9]:

$$\mathrm{Xc}\ (\%) = \frac{\Delta \mathrm{H}_f}{\Delta \mathrm{H}_{f_o}} \times 100 \qquad (1)$$

The symbol ΔHf denotes the fusion enthalpy of the specimens, while ΔHfo corresponds to the conventional enthalpy of polylactic acid, typically assumed to be 93J/g [8]. The experimental apparatus employed for the tests was the NETZSCH-DSC 204 f1 Phoenix equipment (Figure 18).

Figure 18. DSC equipment (NETZSCH-DSC 204 f1 phoenix) used in this work.

4.2.4 Mechanical Characterization

4.2.4.1 Hardness

Shore-D hardness test is a non-destructive technique used to measure the hardness of materials, including composite materials. The Shore-D hardness test measures the resistance of a material to penetration of a spring-loaded needle-like indenter. The test is standardized and widely used in the industry to determine the hardness of soft materials, usually plastic or rubber. The test measures the penetration of a specified indenter into the material under specified conditions of force and time. The hardness value is often used to identify or specify a particular hardness of elastomers or as a quality control measure on lots of material. The data obtained from the test can help engineers understand the mechanical properties of the composite material, which is important for understanding the processing and performance of the composite. The test can also be used to determine the degree of cure of reinforced and non-reinforced rigid plastics [107]. The Shore-D hardness tester is a portable and user-friendly device comprising a dial indicator exhibiting the hardness value on a scale from 0 to 100. The deflection of the instrument's needle indicates the penetration depth of the conical tip, which correlates with the material's hardness under examination. The Shore-D hardness examination is extensively employed in various industries, including the automotive, aerospace, and construction sectors, to evaluate the hardness and caliber of the materials utilized in their commodities [108].

Figure 19. Shore (Durometer) Hardness Tester used in this work.

The Shore D hardness of the samples was assessed utilizing a CV Instruments Limited instrument bearing serial number 6870 (Figure 19) in accordance with the ASTM D2240-00 testing standard. The load was manually applied, and the results were recorded at a sampling rate of 3 Hz. Five experimental trials were conducted on every specimen.

4.2.4.2 Dynamic Modulus of Elasticity Test

The impulse excitation technique (Figure 20) is used to calculate the elastic modulus. The test measures the fundamental resonant frequency of test specimens of suitable geometry by exciting them mechanically with an impulse tool. Five tests were performed on each sample according to the standard ASTM E 1876-01 [109]. The elastic modulus was calculated using Equation 2:

$$E = 0.9465\left(\frac{mft^2}{d}\right)\left(\frac{l^3}{t^3}\right)T_1 \quad (2)$$

Where l, t and d are the dimensions of the sample (length = 60 mm, width = 10 mm, and thickness = 3 mm, respectively), m is the mass and ft is the fundamental frequency of the first flexural vibration mode. Because of the finite dimensions of the samples, a correction factor T_1 is needed. For its calculation, a constant Poisson ratio of 0.3 was assumed.

Figure 20. Dynamic Young's modulus measurement apparatus.

4.2.5 Tribological Characterization

Ball on disc tribological test is a widely used technique to evaluate the wear, friction, and extreme pressure properties of materials, including composite materials. The test consists of a ball under load against a stationery disc. The wear loss of the ball or disc is determined gravimetrically through microscopic examination and surface profiling. The sliding velocities and normal load are controlled to simulate the operating conditions of the material. The ball-on-disc tribological test is a useful tool for evaluating the tribological properties of different composites. The test can provide information about the wear resistance and friction coefficients of various combinations of materials and coatings, sliding properties of self-lubricating bearing materials, and low-friction coatings [110,111]. Three tests were performed on each sample using a pin-on-disk tribometer (RTec) (Figure 21).

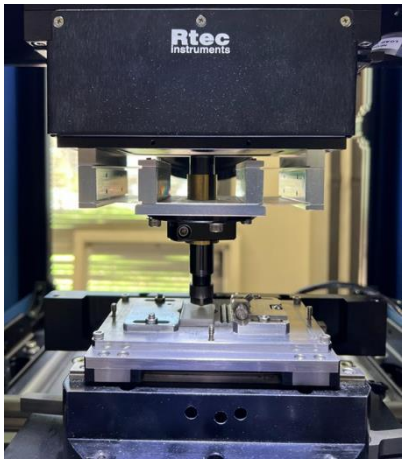

Figure 21. Pin on disk tribometer (Rtec).

A 5N load was exerted via a spherical pin utilizing a stainless steel (100 Cr6) ball measuring 5 mm in diameter. Before initiation, the spherical ball underwent ultrasonic cleansing in ethanol and was subsequently desiccated within the pin holder. It was a test that involved reciprocation. The stroke length was configured to 6 millimeters, the frequency was set to 8.5 Hertz, and the overall time duration was 300 seconds. The experiment was conducted under standard laboratory conditions with a temperature of 25°C and a relative humidity of 50%. Utilizing an Alicona 3D profilometer, an analysis was conducted on the wear track and scar present on the samples. The coefficient denoting the rate of wear, k, was computed utilizing the formula [112]:

$$k = \frac{V}{N}\ (\frac{mm^3}{nm}) \tag{3}$$

The variable V represents the wear volume of the specimen, N denotes the applied load, and S represents the distance traveled.

5. RESULTS AND DISCUSSION

5.1. Raw Materials

The characterization of the raw materials PLA, SCF, and GNP was carried out in a previous study [52] (Figure 22). The PLA granules (Figure 22a) were mostly spherical (equivalent to a diameter of approximately 4.8 mm),

The GNP powder (Figure 22b) presented a flake-like morphology with stacked layers of graphite sheets, and the SCF (Figure 22c) consisted of cylindrical rods with a length of tens of micrometers and diameters lower than 10 μm. Figure 23 shows the optical and SEM images of the PLA and HA raw materials used to produce the PLA, PH-5, and PH-10 filaments. The PLA granules (Figure 23a) had a spherical shape with an equivalent diameter of approximately 4.8 mm. SEM images revealed that the constituent granule size of the HA was typically ≤ 10 μm (Figure 23b). However, there are fair amounts of particles bigger than 10 μm, and the aggregation tendency of the particles was observed during SEM investigation.

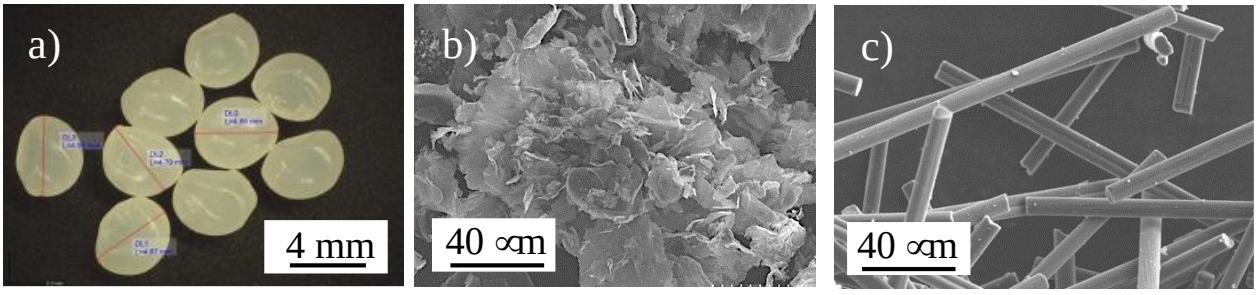

Figure 22. a) Optical image of the PLA granules, b) and c) SEM images of the GNP, and SCF, respectively [52].

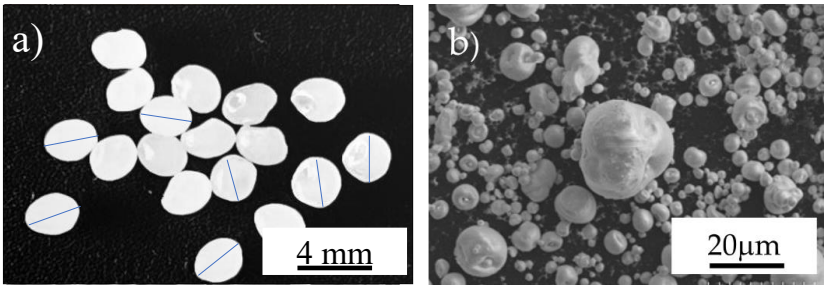

Figure 23. (a) Optical image of the PLA granules, and (b) SEM images of the HA particles.

Figures 24a and b show the XRD patterns of the raw materials used to fabricate the PSG and PH composite system.

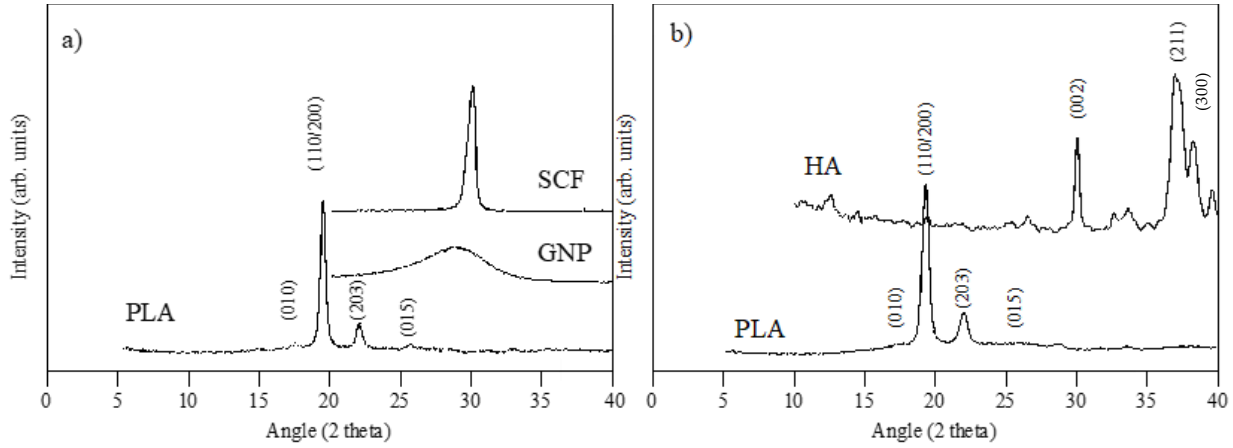

Figure 24. XRD patterns of the raw materials used in this study. (a) PLA, SCF, and GNP [52], and (b) PLA and HA.

The PLA had two intense diffraction peaks at 2θ = 19° and 22°, ascribed to the (200/110) and (203) planes, and two smaller peaks, corresponding to the (010) and (015) diffraction planes of the *α'*-form orthorhombic crystallographic structure [113]. The lattice parameters were calculated from the (010), (200), and (203) planes, and the values of a = 1.06 nm, b = 0.57 nm, and c = 2.85 nm were obtained. In Figure 24a, characteristic diffraction peaks were also illustrated for SCF and GNP. The X-ray diffraction (XRD) analysis of HA depicted in Figure 24b also illustrates three intense peaks at 2θ = 30.04°, 37.08°, and 37.98°, representing the (002), (211), and (300) crystallographic planes, respectively [114].

The DSC curves of the raw PLA used to produce the PSG and PH filaments are shown in Figures 25a and b, respectively. The one used for the PSG samples shows two peaks at 60 and 173° C, corresponding to the glass (Tg) and melting (Tm) temperatures, respectively. The PLA used for the fabrication of the PH samples exhibits the same peaks but shifted to higher temperatures (72 and 183°C). The crystallinity (Xc) of the two PLA granules was calculated using Equation 1, and the values obtained were 45 and 43%, respectively. Therefore, it can be concluded that the two

kinds of PLA granules used are slightly different, which might be due to eventually different chemical compositions, *e.g.*, different numbers of additives.

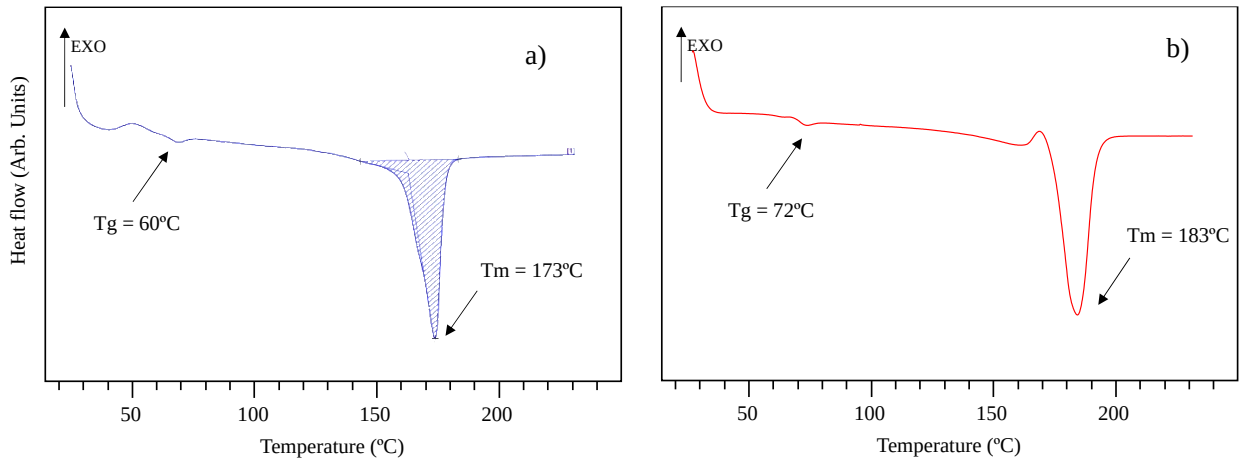

Figure 25. DSC curves of raw PLA used to produce the (a) PSG [52] and (b) PH filaments, respectively.

5.2. Mixture of PLA with the Reinforcements

The torque vs. time curves recorded during the mixture of the raw materials is presented in Figure 26. The maximum torque values occurred in the first seconds of the mixing process and depended on the composition of the samples, i.e., the higher the concentration of SCF and GNP, the higher the maximum torque. This can be explained by the plasticity of the raw materials. Both fillers are ceramic materials with higher hardness and lower ductility than PLA. After 200 s, all the curves became stable and horizontal, meaning that the mixtures were homogenous after that time.

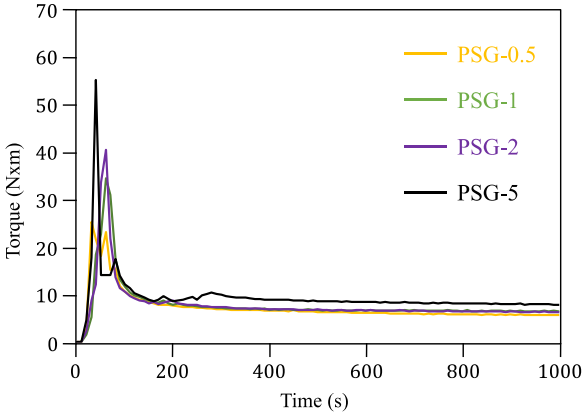

Figure 26. Torque vs. time curves of the reinforced PSG samples.

Considering the time required for the homogenization of PLA and reinforcement materials, HA infill was mixed with PLA for 1800s using the same procedure.

5.3. Production of the Filaments

The mixtures were extruded to produce the filaments and subsequently inspected by optical microscopy. Figures 27a and b show optical images of the PLA and PSG-5 filaments, respectively. They presented some variations in diameter (from 1.75 to 1.94 mm). The average diameter of the filaments was 1.8 mm, suitable for 3D printing. The parts of the filaments with a diameter greater than 1.85 mm were not used to print the samples, to avoid nozzle-clogging issues and to maintain the uniformity of the samples printed. Optical images of the PH-5 and PH-10 filaments are presented in Figures 27c and 27d, respectively. Several diameter variations were observed, ranging from 1.65 to 1.94 mm. Filament sections from each batch (PH-5 and PH-10) closer to the diameter of 1.75 mm were used to print samples considering similar above-mentioned printing challenges.

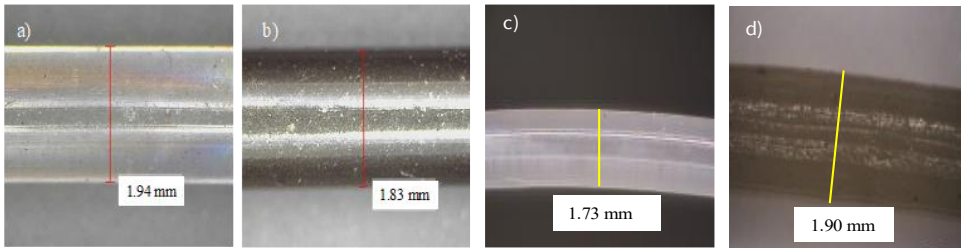

Figure 27. Optical images of the (a) PLA, (b) PSG-5, (c) PH-5, and (d) PH-10 filaments.

During the production of PH filaments, controlling the pellet diameter during the granulation process proved to be difficult, resulting in a collection of granules of different diameters. The filament extrusion process was significantly impacted by this diameter variability, especially when working with PLA and HA fillers. The filament diameter varied because of the granulator machine's variable performance, which led to certain particles melting before others. Figure 28 shows how particles were distributed after granulation. This variation in filament diameter consequently had an immediate impact on the samples' print quality, further jeopardizing their overall consistency.

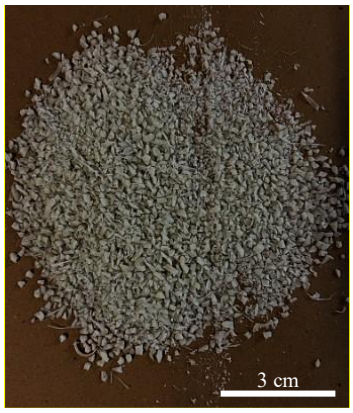

Figure 28. Size distribution of the particles from granulator.

The tomography results of the extruded PLA, PSG-5, and PH-10 filaments are illustrated in Figures 29a, 29b, and 29c, respectively. The filaments were quite dense. The GNP and SCF reinforcements (yellow dots – Figure 29b) were homogeneously distributed throughout the filaments (Figure 29b). The HA fillers were also distributed throughout the filaments of PH samples (Figure 29c)

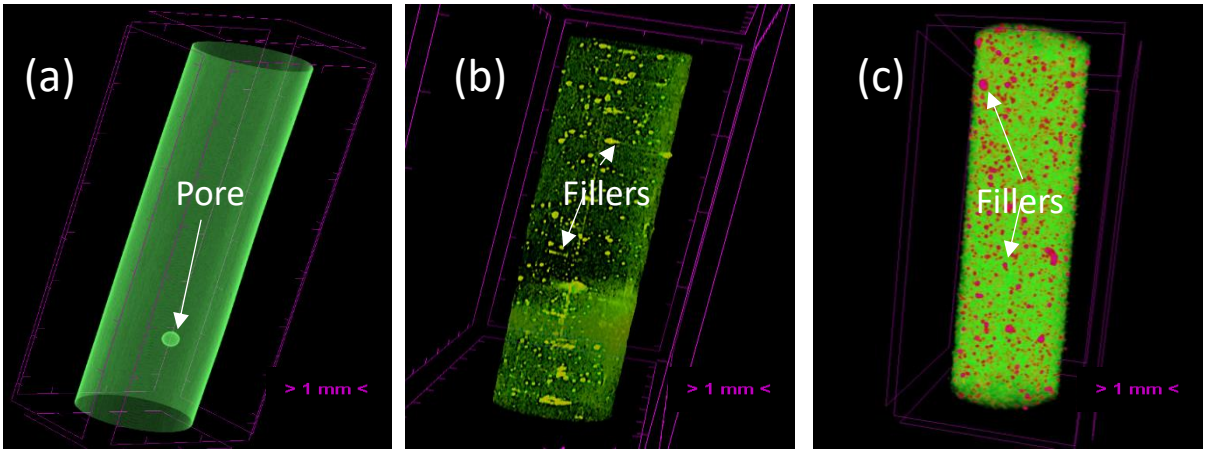

Figure 29. Microtomography images of (a) PLA, (b) PSG-5, and (c) PH-10 filaments - typical examples of all the other filaments.

The DSC curves of PLA and PSG filaments are illustrated in Figure 30a. The curves are identical and characterized by three peaks corresponding to the glass transition (Tg), cold crystallization (Tcc), and melting (Tm) temperatures. The only difference concerned the cold crystallization temperature. The reinforced PLA sample (PSG-5) showed a Tcc value 8°C lower than that of PLA, which suggests SCF and GNP acted as nucleating agents, lowering the crystallization temperature. Similar results were obtained by Ruz-Cruz *et al.* [115] on PLA-based multiscale cellulosic biocomposites and Vinyas *et al.* [116] on PLA + 10% carbon fibers. The existence of Tcc in both DSC curves means that partial amorphization of PLA took place during the processing of the filaments since this peak was not observed for raw PLA [71]. Analogous results were reported

by Sorrentino *et al*. [117]. Similarly, the DSC curves of neat PLA and PH filaments illustrated in Figure 30b are characterized by the same three distinct points, namely, glass transition (Tg), cold crystallization (Tcc), and melting temperatures (Tm). We observe a very slight decrease in the melting peak from 179.9°C to 178.9°C, but it is not relevant [118]. The crystallization temperature of PLA/HA composites reduces all compositions compared to pure PLA. Furthermore, the incorporation of HA into PLA composites leads to a reduction in the glass transition temperature by approximately 5-8°C. This phenomenon may be attributed to the partial breakdown of PLA polymer chains caused by including a highly hydrophilic filler, such as HA. The presence of HA has the potential to induce hydrolysis in certain PLA chains, leading to a plasticization process facilitated by the resulting lactic acid oligomer [119]. Figure 30b illustrates a comparative representation of the DSC curves for PLA/HA composites with varying HA concentrations, enabling the observation of distinct transitions.

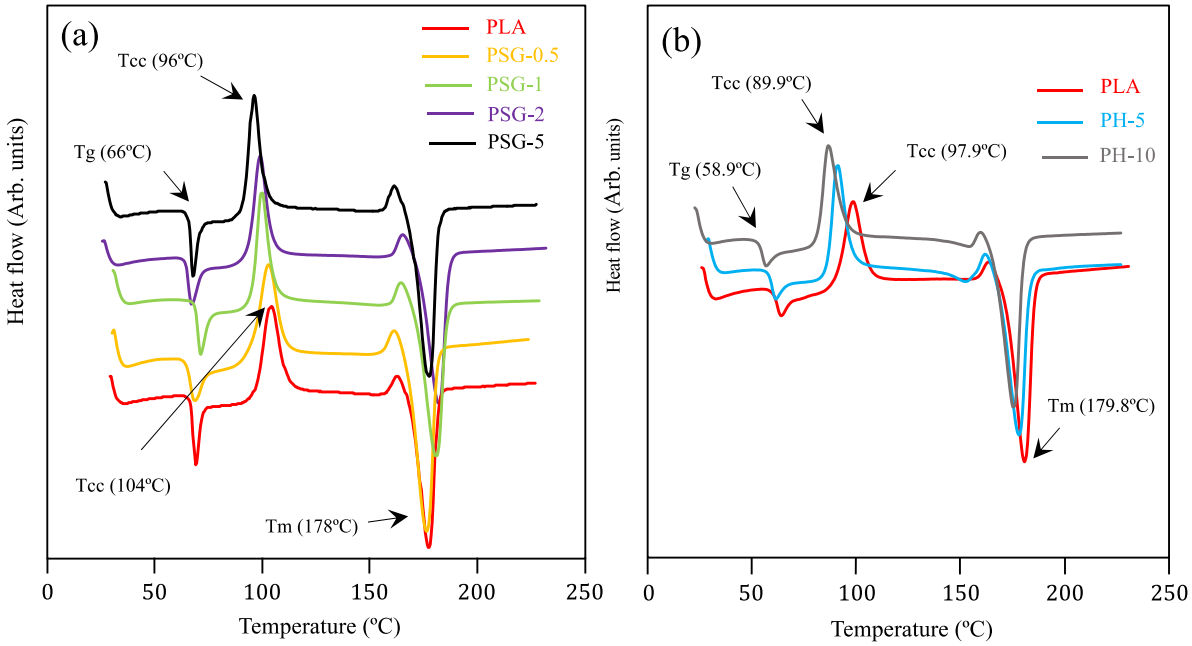

Figure 30. DSC curves of (a) PLA and PSG filaments and (b) PLA and PH filament

5.4. 3D Printed Samples

Figures 31 i) a to f and Figures 31 ii) a to d show SEM images of the PLA and PSG-5 printed samples and PLA and PH-10 samples respectively, to serve as typical examples of all the others. The average thickness of the layers for PSG samples was 200 µm (Figures 31 (i) a and c), while for PH samples, the average layer thickness varied from 350-400 µm (Figures 31 (ii) a and c). A higher porosity was observed at the interface of the composite samples (Figures 31 (i) (b,d) and Figures 31 (ii)b). The images of the surfaces fractured in liquid nitrogen (Figures 31(i) (c and e) revealed a more ductile behavior of the PLA when compared to the composite samples) and partial

separation of the various layers printed in the case of the composite samples. This is related to the fragile behavior of SCF and likely a poor wettability between the PLA matrix and fillers. Triangle-shape voids, which were formed during printing [69,120], were observed on the fracture surface of the PLA samples.

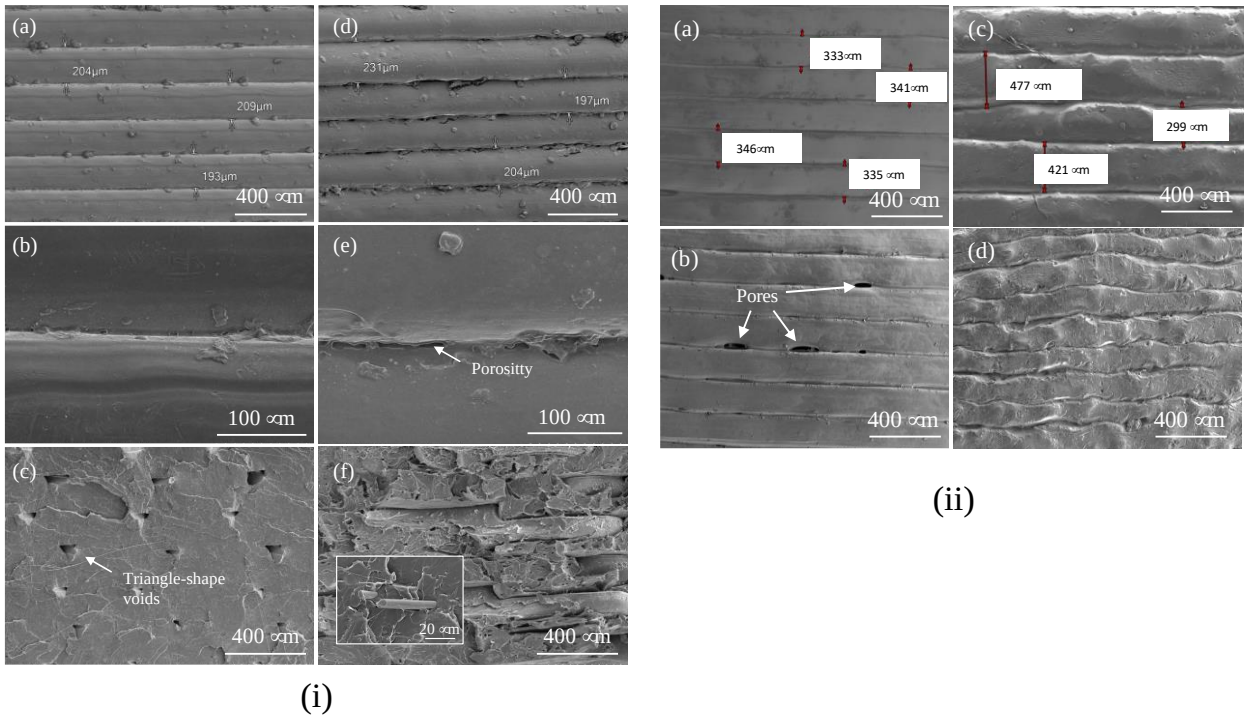

Figure 31. (i) SEM images of (a–c) PLA and (d–f) PGS-5 samples printed. (a,b) Cross-section view, the interface between layers, and (c,f) the fracture surface. The inset in Figure (f) shows a carbon fiber in the PLA matrix. **(ii)** SEM images of (a - b) PLA, and (c-d) PH-10 samples printed.

The XRD patterns of the 3D-printed PLA and PSG samples are shown in Figure 32a. The PLA presented just one broad peak centered at 20º, corresponding to an amorphous structure. During the 3D printing process, the rapid cooling rate impeded the crystallization of PLA. Besides this peak, the reinforced PLA samples also showed diffraction peaks corresponding to the (200/110) plane of PLA (2θ = 19.1°) and graphene (2θ = 30.9°). The intensity of both peaks showed a direct dependence on the concentration of the filler (Figure 33a), meaning that, as mentioned before, SCF and GNP accelerated the crystallization of PLA. Similar results were observed in different studies where other reinforcements were added to PLA [115,116]. The XRD peak of SCF was not detected due to its low intensity and overlapping with the amorphous peak of PLA. The XRD patterns of the 3D-printed PLA and PH samples are shown in Figure 32b. Similarly, the PLA presented just one broad peak centered approximately around 20º, corresponding to an amorphous structure. During the 3D printing process, the rapid cooling rate impeded the crystallization of PLA. Besides this peak, the HA-filled PLA samples also showed double diffraction melt peaks corresponding to the (211) plane of HA with a shoulder (300) at 2θ = 37.04° and 38.39°. The intensity of all these peaks suggests that with the increase of HA content in PLA matrix, the peak intensities are reduced while the characteristic diffraction peaks are more and

more visible (Figure 33b). Similar results were obtained in different studies involving HA into PLA [121,122].

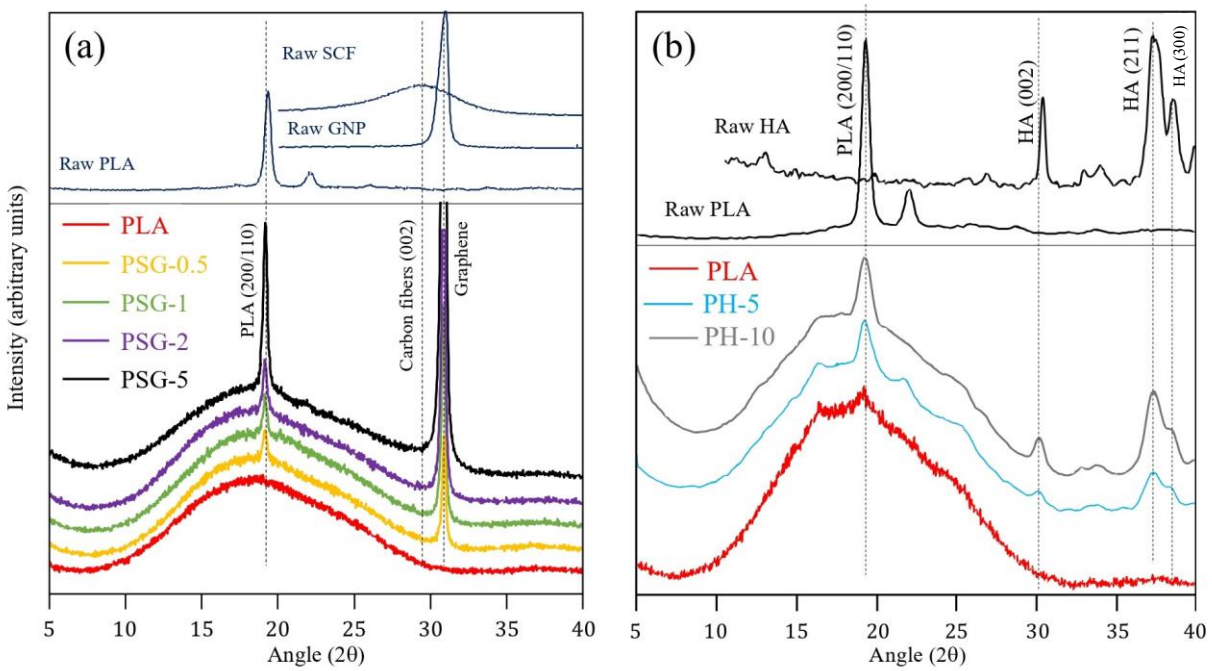

Figure 32. XRD patterns of printed (a) PLA and PSG samples and (b) PLA and PH samples.

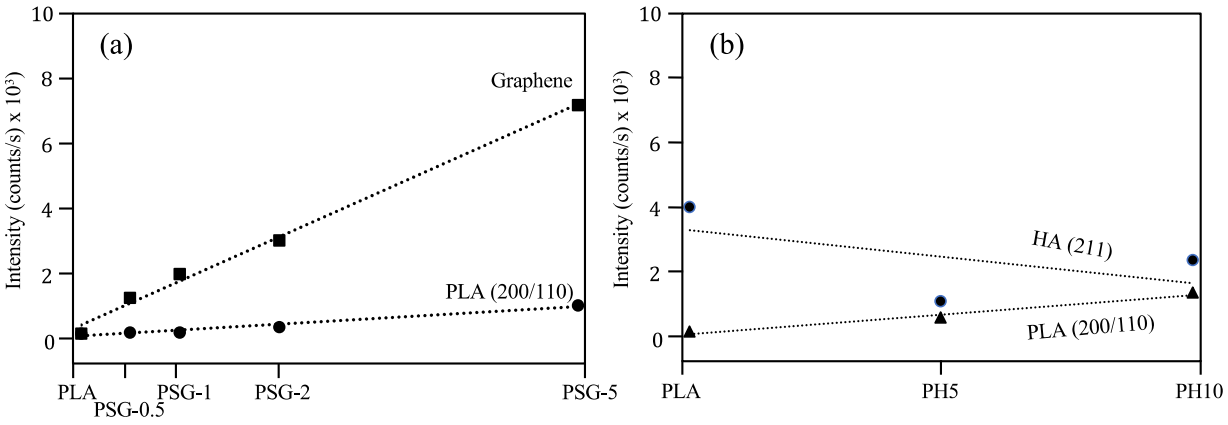

Figure 33. The intensity of (a) PLA (200/110) and graphene diffraction peaks of the samples printed (b) PLA (200/110) and HA diffraction peaks of the samples printed.

The microtomography images of the PLA and PSG-5 samples printed are illustrated in Figure 34, and the microtomography images of the PLA and PH-10 samples printed are illustrated in Figure 35. The 0.2 mm layer-by-layer construction is clearly noticeable (Figure 34a). The 45° raster angle is visible on the surface of the samples (Figures 34a, 34c, 35a, and 35c). The dispersed GNP and SCF particles (yellow dots) were all over the printed sample (Figures 34b and 34c), and the

dispersed HA particles are seen to be distributed (pink dots) all over the printed sample as well (Figures 35b and 35c).

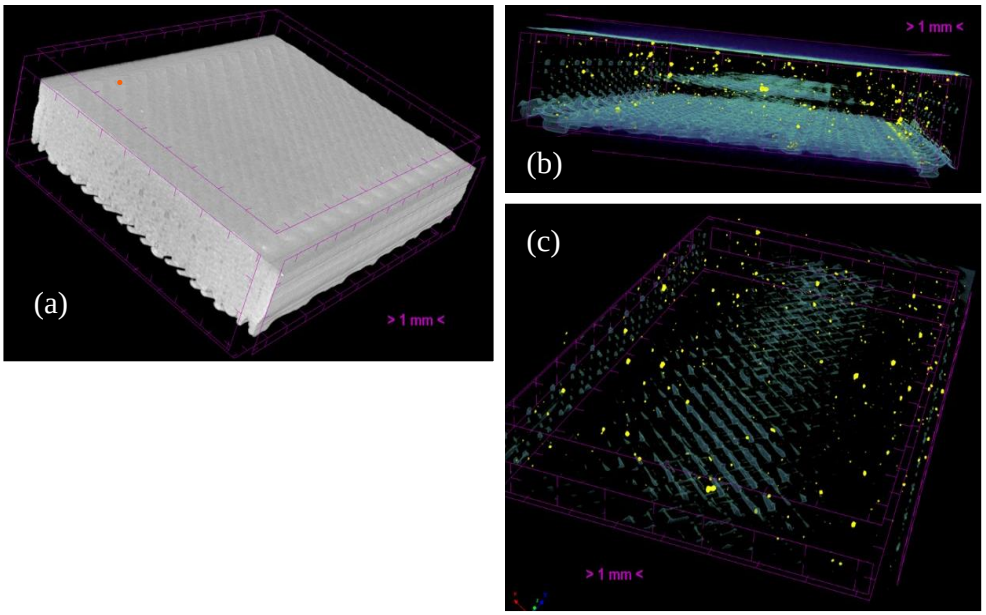

Figure 34. Microtomography images of (a) PLA, (b) PSG-5 (front view) and (c) PSG-5 (isometric view) samples printed.

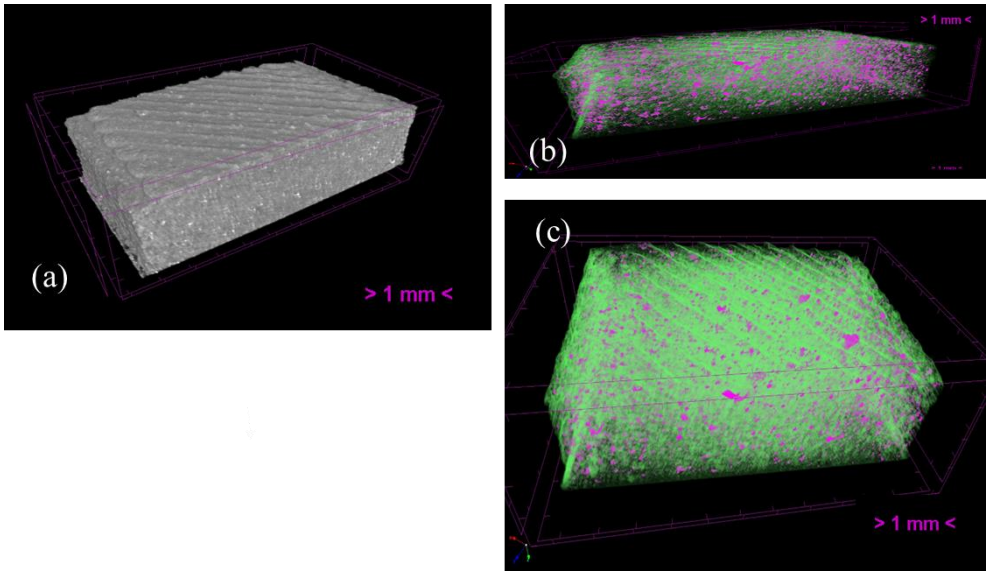

Figure 35. Microtomography images of (a) PH-10, (b) PH-10 (front view) and (c) PH-10 (top view) samples printed.

Table 3 shows the hardness (H), elastic modulus (E), and the H/E ratio of the 3D printed samples (PSG and PH material system). The H/E ratio represents the elastic strain to failure, which is strongly correlated with energy dissipation in mechanical contact. Usually, this relationship is calculated considering the unit of GPa for both properties, H and E. This is not the case in this work, as the hardness was evaluated by the Shore D hardness test. Consequently, the values

should not be compared with the ones from the literature and serve only to establish a relationship between the various samples produced.

Table 3. Hardness (H), elastic modulus (E), and H/E ratio of the 3D printed samples.

PLA/SCF/GNP MATERIAL SYSTEM

SAMPLE	H (shore D)	E (GPa)	H/E
PLA	63.4 ± 0.8	1.86 ± 0.01	33.9
PSG-0.5	77.8 ± 1.0	2.35 ± 0.01	33.2
PSG-1	79.4 ± 0.5	3.14 ± 0.01	25.2
PSG-2	79.2 ± 0.7	3.28 ± 0.02	24.1
PSG-5	81.1 ± 1.0	4.11 ± 0.04	19.7

PLA/HA MATERIAL SYSTEM

SAMPLE	H (shore D)	E (GPa)	H/E
PLA	73.8 ± 0.4	1.9 ± 0.07	38.84
PH-5	76.4 ± 1.0	2.21± 0.04	34.63
PH-10	78.2 ± 0.74	3.83 ± 0.07	20.44

Concerning hardness, the values measured varied from 63.4 and 81.1 Shore D for the PSG material system, while for the PH material system, Shore D values ranged from 73.8 and 78.2. No significant differences in the hardness were detected in the different top surface areas tested, with standard deviation values being quite low.

PLA samples in the PSG material system presented the lowest value (63 Shore D); however, for PH samples, the measured lowest value was (73 Shore D). Since the PLA for both material systems were bought separately, they show differences in their hardness value. The reinforced samples showed higher hardness, with PSG-5 and PH-10 having the highest value (81 Shore D) and (78 Shore D), respectively. The PSG-1 and PSG-2 samples had the same average hardness (79 Shore D), while for PH-5 samples, the measured hardness was (76 Shore D). The hardness of a material depends on its chemical, physical, and mechanical properties. In addition, porosity also contributes to the variation of this property. No significant porosity variation was observed with the addition of carbon fillers or with the addition of HA powders into PLA. Therefore, the addition of GNP and SCF to PLA, and in the case of PH samples, the addition of HA was responsible for the increase in hardness. It is reported in the literature that even a small amount of GNP and SCF can boost the hardness of polymer-based composites [20,123-125]. This happens because both fillers are harder than PLA. On the other hand, researchers have stated that HA particles improve the overall hardness of the material system when incorporated into polymer matrices [83,126].

Regarding the elastic modulus, the values increased as the concentration of the fillers in the PLA matrix increased. The PLA presented an elastic modulus of 1.86 GPa for PSG samples and 1.9 GPa for PH samples; these values are slightly higher than the one reported by Leite *et al*. [127]. However, the values are lower than the typical elastic modulus of commercial PLA obtained by traditional processes (3.5 GPa) [128,129] due to the low crystallinity and high number of pores of the 3D-printed PLA. As observed for hardness, the addition of just 0.5 wt.% of SCF and 0.5 wt.% of GNP significantly increased the elastic modulus (2.35 GPa). On the other hand, in PH samples,

with the addition of 5 wt.% HA, the modulus of elasticity reached 2.21 GPa. Samples with 1 wt.% and 2 wt.% of both fillers showed similar elastic moduli of 3.14 GPa (PSG-1) and 3.28 GPa (PSG-2). The highest value (4.11 GPa) was obtained for the PSG-5 sample, and with the PH-10 sample (highest concentration of fillers), 3.82 GPa was obtained as their elastic modulus of elasticity. These results are in accordance with previous studies on PLA-based composites reinforced with GNP or SCF [28,59,130-133] and PLA-based composites reinforced with HA or other ceramic fillers [134-136]. These reinforcements have a higher tensile strength and elastic modulus than PLA, which restricts the movement of the polymeric chains, leading to improved resistance to strain and an increased load-bearing capacity. As a result, the reinforced PLA samples can resist the loads applied more effectively than only PLA.

As expected, the H/E ratios of the samples printed showed a decrease with the increase in the concentration of fillers. As mentioned before, the addition of GNP and SCF to PLA and HA to PLA increased both H and E. However, its influence on E was predominant, and therefore, the elastic strain to breakage is decreased by increasing the content of fillers in PLA.

The CoF curves of the 3D-printed samples from the PSG system are presented in Figure 36a. Small amounts of SCF and GNP (0.5 wt.%) were enough to significantly reduce the CoF. All the composite samples showed lower CoF values (0.49 to 0.6) compared to PLA (0.71). The PSG-0.5 and PSG-1 samples had the lowest value (~ 0.49) among all the composite samples. The further increase in SCF and GNP contents (2 wt.% and 5 wt.%) led to an increase of CoF (0.6). These results are in tune with the ones reported by Hanon *et al*. [132], although the polymer was different (polyurethane-based resin) in that study, and only graphene was used as the reinforcement. During the reciprocating ball-on-disk tests, the carbon flakes provided a transfer of the film that acted as a solid lubricant [137], reducing the CoF of PLA [138]. The addition of high concentrations of fillers (mainly SCF) gave rise to harder and less flexible composites. As the fibers did not bend as easily in contact with the counter body, this led to more friction. Moreover, SCF presented more surface asperities, which may also cause more friction. For the 3D-printed samples from the PH material system, the addition of 5 wt.% HA into PLA reduced its CoF value from 0.57 to 0.49 (figure 36b). The further addition of HA didn't have any effect in changing COF value compared to PH-5. Hence, the lowest CoF value for this material system was obtained when 5wt.% of HA was used as a filler into PLA matrix.

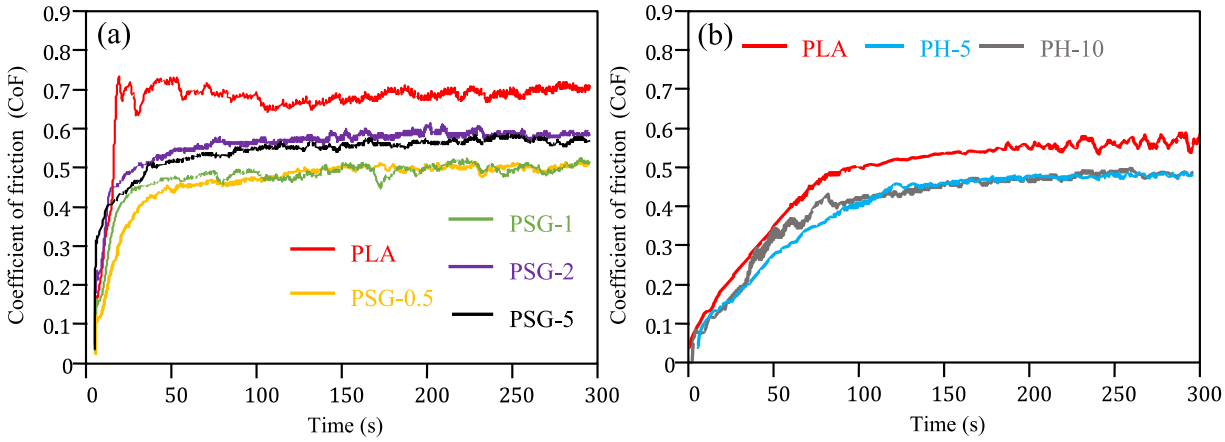

Figure 36. CoF curves of the 3D printed samples (a) PSG material system (b) PH material system.

Figure 37a shows the 3D profilometry images of the printed samples' (PSG) wear profiles. The corresponding specific wear rates are illustrated in Figure 38a. All the composite samples presented lower wear depths than the PLA. The PSG-5 sample showed the lowest value (11 μm), much lower than PLA (50 μm). The PSG-0.5 and PSG-1 samples had similar values, close to 15-16 μm. The PSG-2 sample had the highest maximum wear depth (18 μm) among them. Figure 37b shows the 3D profilometry images of the printed samples' (PH) wear profiles. Their corresponding specific wear rates are illustrated in Figure 38b. All the composite samples presented lower wear depths than the PLA. The PH-10 sample showed the lowest value (9 μm), lower than PLA (20 μm). The PH-5 and PH-10 samples had similar values, close to 9-11 μm.

Figure 38 shows the wear rate of 3D Printed samples. In PSG samples, the PLA presented a specific wear rate of 2.1 x 10^{-3} mm^3/N.m. The incorporation of SCF + GNP into PLA led to a decreased wear rate. The lowest value was obtained for the PSG-5 sample (4.04 x 10^{-4} mm^3/N.m), corresponding to about 5 times reduction compared to PLA. All the other composite samples showed lower specific wear rates (from 6.14 x 10^{-3} to 7.47 x 10^{-3} mm^3/N.m) than PLA but higher than PSG-5. Similar results were obtained by Bustillos *et al*. [78] for GNP-reinforced PLA. In PH samples, PLA presented a specific wear rate of 4.82 x 10^{-4} mm^3/N.m. The incorporation of HA into PLA led to a decreased wear rate. The lowest value was obtained for the PH-10 sample (2.75 x 10^{-4} mm^3/N.m), corresponding to about 1.8 times reduction compared to PLA. PH-5 and PH-10 samples had similar specific wear rates ranging from (2.73-2.86) x 10^{-4} mm^3/N.m. Similar results were obtained by Macuvele *et al*.[126] for UHMWPE/HA composite.

Friedrich [139] also demonstrated that SCF can significantly improve the wear resistance of PEEK+ PTFE (polytetrafluoroethylene) engineered plastics. Both the SCF and GNP are harder than PLA, which increases the composites' hardness and wear resistance. Additionally, SCF increases the region of contact surface with higher load-bearing capacity, providing these composites with higher wear resistance. During the sliding wear tests, there is a high probability that these particles will be released by the composites and roll between the sliding surfaces.

Subsequently, they act as solid lubricants, minimizing the contact points between the counter bodies and the surface of the composites, which leads to lowered CoF and wear [27,137]. Moreover, the SCF and GNP fillers reduce the concentration of stress during the wear tests and the formation of a network of microcracks, resulting in a dramatic decrease in wear [140]. The carbon fibers act as a reinforcement phase, capable of distributing the load over a larger area. This helps reduce the concentration of stress at the surface and increases the material's wear resistance. Additionally, the carbon fibers act as a barrier to prevent the polymer matrix from deforming, which also improves the material's wear resistance. With increasing carbon content, the hardness and elastic modulus of the composites also increase, which means they can withstand large loads without breaking or deforming. As a result, overall improvements of the composite materials' (PSG) mechanical properties help to increase the wear resistance. In PH samples, it was demonstrated that adding HA to the PLA matrix enhances its tribological capabilities. There hasn't been a study done yet that investigates this phenomenon. However, contemporary research has examined the effects of adding HA to polymer composites, and a consensus has evolved about its favorable impact on wear properties [141]. This discovery is in line with the findings of current research. According to Kang *et al.* [85], the reason why wear rates are reduced when HA is introduced to UHMPWE is that the filler particles—in this case, HA—behave as stiff points against the opposing surface, which is frequently comprised of metal. The normal load and shear stress placed on the polymer is reduced because of this interaction, which lowers the rate of wear. The research of Schwartz *et al.* [142] and Xiong *et al.* [82] lends credence to this notion. It is important to note that the wear of materials is inextricably tied to both their mechanical characteristics, such as their modulus, and the fabrication processes used to create them [84].

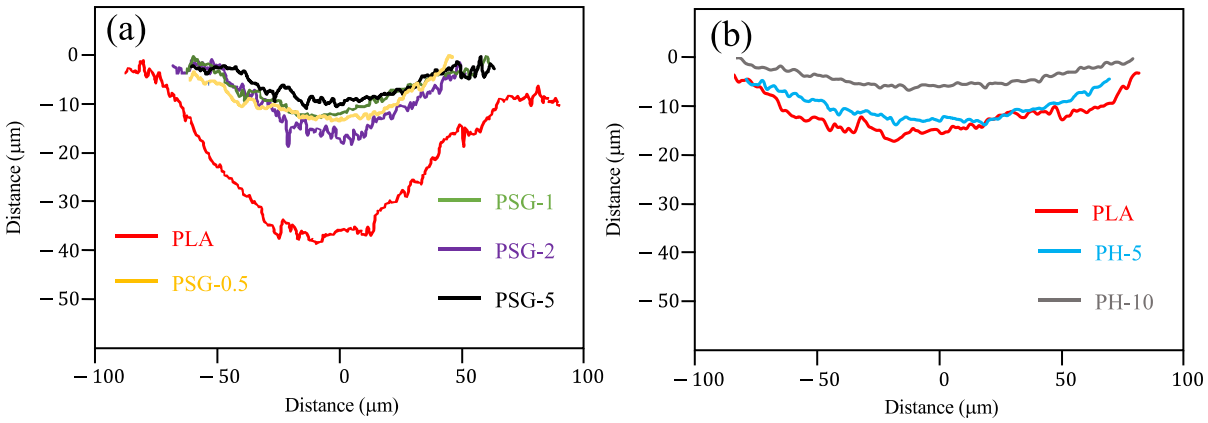

Figure 37. Wear profiles of the 3D printed (a) PSG samples and (b) PH samples.

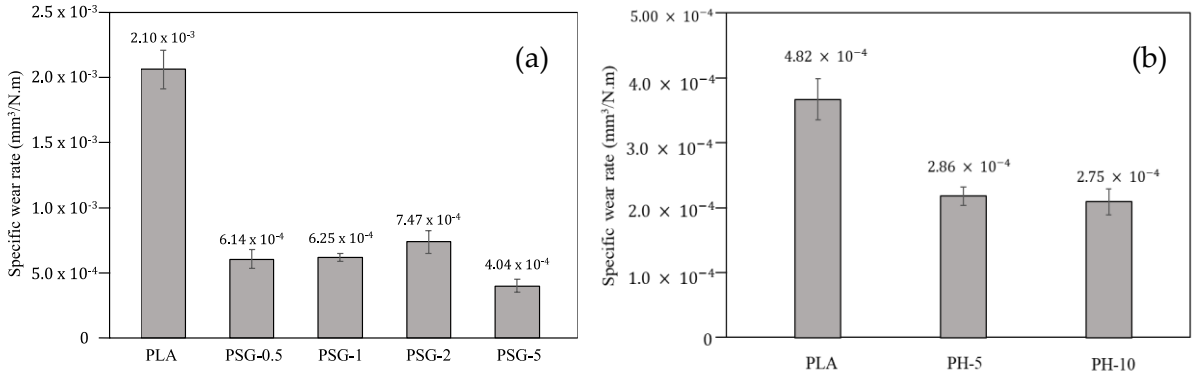

Figure 38. Specific wear rates of the 3D printed (a) PSG samples and (b) PH samples.

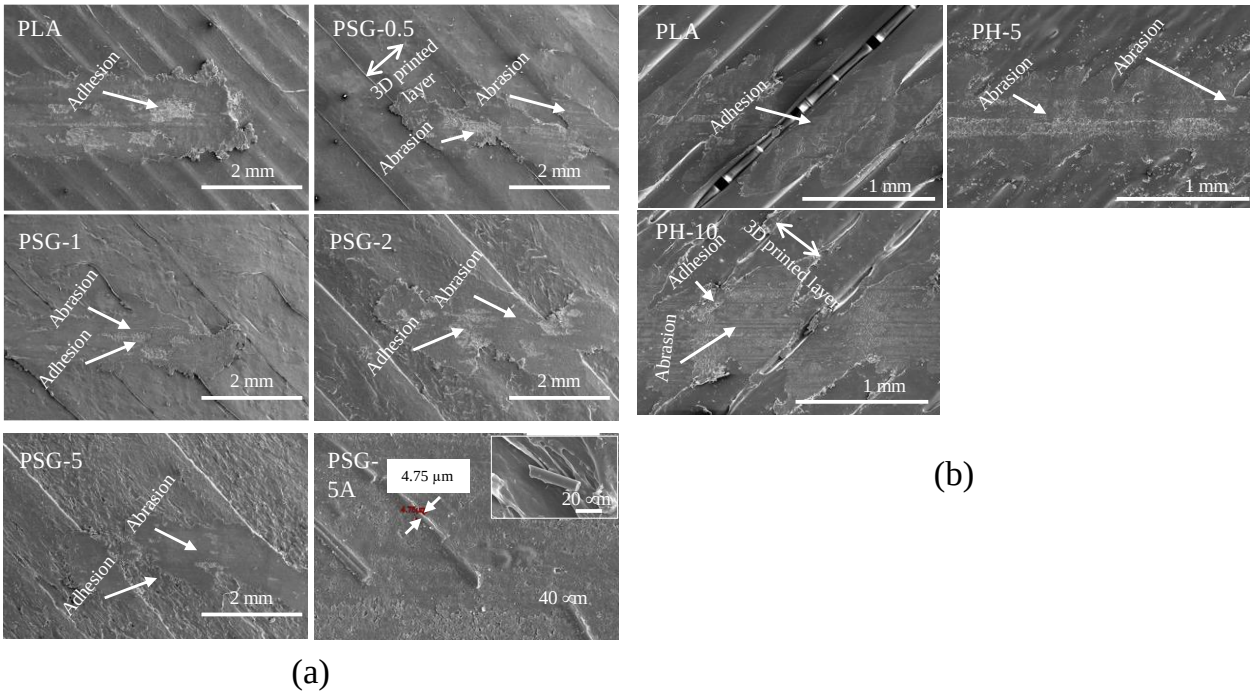

Figure 39. SEM images of the wear scars on the 3D printed (a) PLA and PSG samples and (b) PLA and PH samples after the tribological tests.

The wear mechanisms on the worn surfaces were characterized using SEM (Figure 39). The worn surface of the PLA in both samples mostly demonstrated the adhesive wear mechanism that led to wear debris emerging because of an adhesion process caused by plastic deformation and shear. This conclusion is consistent with Lancaster's work [143].

Abrasion, along with adhesion, was the most common wear process in all the reinforced PLA composites. In PSG samples, SCF particles emerged on top of the composite surfaces during the sliding of the steel counter body on them (Figure 39 - PSG-5A). The wear of the composites was mainly due to a three-body abrasive wear mechanism. A similar phenomenon has already been documented in other studies [78,131]. The SCF assisted in supporting the applied load and

protected the PLA matrix from wear. GNP acted as a solid lubricant, reducing the direct contact between the steel balls and the PLA matrix, thus preventing easy removal of the polymeric matrix. This explains why the wear was significantly lower in the composites compared to PLA in PSG samples. In the case of the PH sample, HA particles acted as a rigid contact point against the counter body resulting in improvement in wear and friction behavior [85].

Finally, one may say that the increase in the fillers content (from 0.5 to 5 wt.%) in PSG samples was responsible for the increase in the mechanical properties and load-bearing capacity and the decrease in the plastic deformation, which led to the enhanced specific wear resistance of the composites. Although samples of PLA reinforced with only one kind of mono filler were not produced in the case of PSG samples, it is possible to state that the results are in line with a previous study on the fabrication of PLA bio-composites by mechanical alloying and casting [52]. That is, there was a combined effect of the solid lubrication of graphene and the increase in hardness and elastic modulus achieved by SCF. In PH samples, although the variation in mechanical and tribological properties took a positive turn with the incorporation of HA into the polymer matrix, there wasn't a significant improvement in properties when HA content was increased from 5wt.% to 10 wt.%. To understand better the effect of filler content variation in PH materials it is recommended to investigate PLA filled with 15 wt.% HA in PH composites.

6. CONCLUSIONS

The results of this study allowed us to draw the following conclusions:

- The manufacturing process employed in this study successfully produced filaments with a well-dispersed distribution of SCF, GNP, and HA. This effective dispersion of fillers within the PLA matrix is a crucial factor in enhancing the mechanical and tribological properties of the composite material. A noticeable increase in the hardness and elastic modulus of the PLA composite occurred as a result.
- The incorporation of these fillers into the PLA matrix contributed to solid lubrication properties, which are vital for reducing friction and wear between moving surfaces. The fillers acted as solid lubricants within the composite material, facilitating smoother sliding and reducing frictional forces. This solid lubrication effect greatly enhances the tribological performance of the PLA composite, rendering it particularly suitable for applications where low friction and exceptional wear resistance are of utmost importance.
- The mechanical and tribological properties exhibited by the PSG and PH samples were found to be directly dependent on the filler content. The variation in filler content allowed for the fine-tuning of these properties, providing insights into the optimal composition for achieving desired mechanical strength, stiffness, and wear resistance. This dependence highlights the importance of carefully controlling the filler content when designing PLA-based composite materials with specific mechanical and tribological requirements.
- The PSG-5 sample (5 wt.% of SCF and 5 wt.% of GNP) showed a 30% increase in hardness compared to unreinforced PLA (81.1 and 33.4 Shore D, respectively) and a 220% increase in modulus of elasticity (4.11 and 1.86 GPa, respectively). On the other hand, the PH-10 sample (5 wt.% of PLA and 10 wt.% of HA) showed a 6% increase in hardness compared to unreinforced PLA (78.2 and 73.8 Shore D, respectively) and a 202% increase in modulus of elasticity (3.83 and 1.9 GPa, respectively). However, a further investigation with 15wt.% HA should be done to draw similar conclusions about PH samples.
- Regarding the tribological behavior, the reinforced PLA samples showed lower friction coefficients than the non-reinforced PLA, as well as a decrease in the specific wear rate. The PSG-5 sample from PSG samples had the lowest value (4.04×10^{-4} $mm^3/N.m$), corresponding to about 5 times reduction compared to PLA, while PH-10 sample from PH samples showed a 1.8 times reduction in wear (4.04×10^{-4} $mm^3/N.m$) than PLA.
- Finally, the PLA-based composites produced in this work are promising materials for biomedical applications, e.g., manufacturing of improved PLA-based scaffolds and implants.

REFERENCES

[1] O. Diegel, "10.02 - Additive Manufacturing: An Overview," S. Hashmi, G. F. Batalha, C. J. Van Tyne, and B. B. T.-C. M. P. Yilbas, Eds. Oxford: Elsevier, 2014, pp. 3–18. doi: https://doi.org/10.1016/B978-0-08-096532-1.01000-1.

[2] O. A. Mohamed, S. H. Masood, and J. L. Bhowmik, "Optimization of fused deposition modeling process parameters: a review of current research and future prospects," *Adv. Manuf.*, vol. 3, no. 1, pp. 42–53, 2015, doi: 10.1007/s40436-014-0097-7.

[3] N. Hossain, M. A. Chowdhury, M. B. A. Shuvho, M. A. Kashem, and M. Kchaou, "3D-Printed Objects for Multipurpose Applications," *J. Mater. Eng. Perform.*, vol. 30, no. 7, pp. 4756–4767, 2021, doi: 10.1007/s11665-021-05664-w.

[4] A. Jandyal, I. Chaturvedi, I. Wazir, A. Raina, and M. I. Ul Haq, "3D printing – A review of processes, materials and applications in industry 4.0," *Sustain. Oper. Comput.*, vol. 3, pp. 33–42, 2022, doi: https://doi.org/10.1016/j.susoc.2021.09.004.

[5] A. A. Mohammed, M. S. Algahtani, M. Z. Ahmad, J. Ahmad, and S. Kotta, "3D Printing in medicine: Technology overview and drug delivery applications," *Ann. 3D Print. Med.*, vol. 4, p. 100037, 2021, doi: https://doi.org/10.1016/j.stlm.2021.100037.

[6] A. Hayes and K. Khartit, "3D Printing: What It Is, How It Works, Examples," *Investopedia*, 2021. https://www.investopedia.com/terms/1/3d-printing.asp (accessed Jun. 12, 2023).

[7] H. Tetsuka and S. R. Shin, "Materials and technical innovations in 3D printing in biomedical applications.," *J. Mater. Chem. B*, vol. 8, no. 15, pp. 2930–2950, Apr. 2020, doi: 10.1039/d0tb00034e.

[8] P. Ahangar, M. E. Cooke, M. H. Weber, and D. H. Rosenzweig, "Current Biomedical Applications of 3D Printing and Additive Manufacturing," *Applied Sciences*, vol. 9, no. 8. 2019. doi: 10.3390/app9081713.

[9] Y. Bozkurt and E. Karayel, "3D printing technology; methods, biomedical applications, future opportunities and trends," *J. Mater. Res. Technol.*, vol. 14, pp. 1430–1450, 2021, doi: https://doi.org/10.1016/j.jmrt.2021.07.050.

[10] "3D Printing Medical Devices Market," *Fact.Mr*, 2022. https://www.factmr.com/report/248/3d-printing-medical-devices-market (accessed Jun. 12, 2023).

[11] "Healthcare 3D Printing Market - By Product," *Global Market Insights*, 2022. https://www.gminsights.com/industry-analysis/healthcare-3D-printing-market (accessed Jun. 12, 2023).

[12] "3D Printing in Healthcare Market," *Precedence Research*, 2022. https://www.precedenceresearch.com/3d-printing-in-healthcare-market (accessed Jun. 12, 2023).

[13] S. Saleh Alghamdi, S. John, N. Roy Choudhury, and N. K. Dutta, "Additive Manufacturing of Polymer Materials: Progress, Promise and Challenges.," *Polymers (Basel).*, vol. 13, no. 5, Feb. 2021, doi: 10.3390/polym13050753.

[14] A. M. R. Group, "About Additive Manufacturing," *Loughborough University*. https://www.lboro.ac.uk/research/amrg/about/materials/

[15] A. Nazir *et al.*, "Multi-material additive manufacturing: A systematic review of design, properties, applications, challenges, and 3D printing of materials and cellular metamaterials," *Mater. Des.*, vol. 226, p. 111661, 2023, doi: https://doi.org/10.1016/j.matdes.2023.111661.

[16] R. Donate, M. Monzón, and M. E. Alemán-Domínguez, "Additive manufacturing of PLA-based scaffolds intended for bone regeneration and strategies to improve their biological properties," vol. 20, no. 1, pp. 571–599, 2020, doi: doi:10.1515/epoly-2020-0046.

[17] R. M. Rasal, A. V Janorkar, and D. E. Hirt, "Poly(lactic acid) modifications," *Prog. Polym. Sci.*, vol. 35, no. 3, pp. 338–356, 2010, doi: https://doi.org/10.1016/j.progpolymsci.2009.12.003.

[18] P. Saini, M. Arora, and M. N. V. R. Kumar, "Poly(lactic acid) blends in biomedical applications," *Adv. Drug Deliv. Rev.*, vol. 107, pp. 47–59, 2016, doi: https://doi.org/10.1016/j.addr.2016.06.014.

[19] M. Ivey, G. W. Melenka, J. P. Carey, and C. Ayranci, "Characterizing short-fiber-reinforced composites produced using additive manufacturing," *Adv. Manuf. Polym. Compos. Sci.*, vol. 3, no. 3, pp. 81–91, Jul. 2017, doi: 10.1080/20550340.2017.1341125.

[20] Z. Z. Wang, P. Gu, and Z. Zhang, "Indentation and scratch behavior of nano-SiO2/polycarbonate composite coating at the micro/nano-scale," *Wear*, vol. 269, no. 1, pp. 21–25, 2010, doi: https://doi.org/10.1016/j.wear.2010.03.003.

[21] I. S. Bayer, "Thermomechanical Properties of Polylactic Acid-Graphene Composites: A State-of-the-Art Review for Biomedical Applications.," *Mater. (Basel, Switzerland)*, vol. 10, no. 7, Jul. 2017, doi: 10.3390/ma10070748.

[22] C. Gonçalves, A. Pinto, A. V. Machado, J. Moreira, I. C. Gonçalves, and F. Magalhães, "Biocompatible reinforcement of poly(Lactic acid) with graphene nanoplatelets," *Polym. Compos.*, vol. 39, no. S1, pp. E308–E320, Apr. 2018, doi: https://doi.org/10.1002/pc.24050.

[23] K. Prashantha and F. Roger, "Multifunctional properties of 3D printed poly(lactic acid)/graphene nanocomposites by fused deposition modeling," *J. Macromol. Sci. Part A*, vol. 54, no. 1, pp. 24–29, Jan. 2017, doi: 10.1080/10601325.2017.1250311.

[24] A.-D. Lin and J.-H. Kuang, "Dynamic interaction between contact loads and tooth wear of engaged plastic gear pairs," *Int. J. Mech. Sci.*, vol. 50, no. 2, pp. 205–213, 2008, doi: https://doi.org/10.1016/j.ijmecsci.2007.07.002.

[25] R. Rabinowicz, *Friction and Wear of Materials*, 2nd ed. Wiley, 1995.

[26] K. Friedrich, Z. Zhang, and A. K. Schlarb, "Effects of various fillers on the sliding wear of

polymer composites," *Compos. Sci. Technol.*, vol. 65, no. 15, pp. 2329–2343, 2005, doi: https://doi.org/10.1016/j.compscitech.2005.05.028.

[27] N. W. KHUN, H. ZHANG, L. H. LIM, C. Y. YUE, X. HU, and J. YANG, "Tribological properties of short carbon fibers reinforced epoxy composites," *Friction*, vol. 2, no. 3, pp. 226–239, 2014, doi: 10.1007/s40544-014-0043-5.

[28] M. Á. Caminero, J. M. Chacón, E. García-Plaza, P. J. Núñez, J. M. Reverte, and J. P. Becar, "Additive Manufacturing of PLA-Based Composites Using Fused Filament Fabrication: Effect of Graphene Nanoplatelet Reinforcement on Mechanical Properties, Dimensional Accuracy and Texture," *Polymers*, vol. 11, no. 5. 2019. doi: 10.3390/polym11050799.

[29] K. S. Novoselov *et al.*, "Electric Field Effect in Atomically Thin Carbon Films," *Science (80-.).*, vol. 306, no. 5696, pp. 666–669, Oct. 2004, doi: 10.1126/science.1102896.

[30] H. Quan, B. Zhang, Q. Zhao, R. K. K. Yuen, and R. K. Y. Li, "Facile preparation and thermal degradation studies of graphite nanoplatelets (GNPs) filled thermoplastic polyurethane (TPU) nanocomposites," *Compos. Part A Appl. Sci. Manuf.*, vol. 40, no. 9, pp. 1506–1513, 2009, doi: https://doi.org/10.1016/j.compositesa.2009.06.012.

[31] E. Fiume, G. Magnaterra, A. Rahdar, E. Verné, and F. Baino, "Hydroxyapatite for Biomedical Applications: A Short Overview," *Ceramics*, vol. 4, no. 4. pp. 542–563, 2021. doi: 10.3390/ceramics4040039.

[32] M.-P. Ginebra, M. Espanol, Y. Maazouz, V. Bergez, and D. Pastorino, "Bioceramics and bone healing.," *EFORT open Rev.*, vol. 3, no. 5, pp. 173–183, May 2018, doi: 10.1302/2058-5241.3.170056.

[33] A. Södergård and M. Stolt, "Properties of lactic acid based polymers and their correlation with composition," *Prog. Polym. Sci.*, vol. 27, no. 6, pp. 1123–1163, 2002, doi: https://doi.org/10.1016/S0079-6700(02)00012-6.

[34] S. Jacobsen and H. G. Fritz, "Filling of poly(lactic acid) with native starch," *Polym. Eng. Sci.*, vol. 36, no. 22, pp. 2799–2804, Nov. 1996, doi: https://doi.org/10.1002/pen.10680.

[35] A. Mohanty, M. Misra, L. Drzal, S. Selke, B. Harte, and G. Hinrichsen, "Natural Fibers, Biopolymers, And Biocomposites," in *Soy Protein-based Plastics, Blends, and Composites*, vol. 1, 2005, pp. 1–36. doi: 10.1201/9780203508206.

[36] S. Farah, D. G. Anderson, and R. Langer, "Physical and mechanical properties of PLA, and their functions in widespread applications — A comprehensive review," *Adv. Drug Deliv. Rev.*, vol. 107, pp. 367–392, 2016, doi: https://doi.org/10.1016/j.addr.2016.06.012.

[37] K. Modjarrad and S. B. T.-H. of P. A. in M. and M. D. Ebnesajjad, Eds., "Copyright," in *Plastics Design Library*, Oxford: William Andrew Publishing, 2014, p. iv. doi: https://doi.org/10.1016/B978-0-323-22805-3.00016-5.

[38] J. Lunt, "Large-scale production, properties and commercial applications of polylactic acid polymers," *Polym. Degrad. Stab.*, vol. 59, no. 1, pp. 145–152, 1998, doi: https://doi.org/10.1016/S0141-3910(97)00148-1.

[39] A. J. Svagan *et al.*, "Transparent Films Based on PLA and Montmorillonite with Tunable Oxygen Barrier Properties," *Biomacromolecules*, vol. 13, no. 2, pp. 397–405, Feb. 2012, doi: 10.1021/bm201438m.

[40] J. C. Middleton and A. J. Tipton, "Synthetic biodegradable polymers as orthopedic devices," *Biomaterials*, vol. 21, no. 23, pp. 2335–2346, 2000, doi: https://doi.org/10.1016/S0142-9612(00)00101-0.

[41] G. Mensitieri *et al.*, "Processing and shelf life issues of selected food packaging materials and structures from renewable resources," *Trends Food Sci. Technol.*, vol. 22, no. 2, pp. 72–80, 2011, doi: https://doi.org/10.1016/j.tifs.2010.10.001.

[42] K. J. Jem and B. Tan, "The development and challenges of poly (lactic acid) and poly (glycolic acid)," *Adv. Ind. Eng. Polym. Res.*, vol. 3, no. 2, pp. 60–70, 2020, doi: https://doi.org/10.1016/j.aiepr.2020.01.002.

[43] A. V Janorkar, A. T. Metters, and D. E. Hirt, "Modification of Poly(lactic acid) Films: Enhanced Wettability from Surface-Confined Photografting and Increased Degradation Rate Due to an Artifact of the Photografting Process," *Macromolecules*, vol. 37, no. 24, pp. 9151–9159, Nov. 2004, doi: 10.1021/ma049056u.

[44] M. Keck, D. B. Lumenta, and L.-P. Kamolz, "Generation of adipose tissue based on tissue engineering: An overview BT - Handbook of Burns: Reconstruction and Rehabilitation Volume 2," L.-P. Kamolz, M. G. Jeschke, R. E. Horch, M. Küntscher, and P. Brychta, Eds. Vienna: Springer Vienna, 2012, pp. 181–188. doi: 10.1007/978-3-7091-0315-9_15.

[45] K. Hamad, M. Kaseem, M. Ayyoob, J. Joo, and F. Deri, "Polylactic acid blends: The future of green, light and tough," *Prog. Polym. Sci.*, vol. 85, pp. 83–127, 2018, doi: https://doi.org/10.1016/j.progpolymsci.2018.07.001.

[46] M. Nofar, D. Sacligil, P. J. Carreau, M. R. Kamal, and M.-C. Heuzey, "Poly (lactic acid) blends: Processing, properties and applications," *Int. J. Biol. Macromol.*, vol. 125, pp. 307–360, 2019, doi: https://doi.org/10.1016/j.ijbiomac.2018.12.002.

[47] M. Ramesh, L. N. Rajeshkumar, N. Srinivasan, D. V. Kumar, and D. Balaji, "Influence of filler material on properties of fiber-reinforced polymer composites: A review," vol. 22, no. 1, pp. 898–916, 2022, doi: doi:10.1515/epoly-2022-0080.

[48] A. Amjad, A. Anjang Ab Rahman, H. Awais, M. S. Zainol Abidin, and J. Khan, "A review investigating the influence of nanofiller addition on the mechanical, thermal and water absorption properties of cellulosic fibre reinforced polymer composite," *J. Ind. Text.*, vol. 51, no. 1_suppl, pp. 65S-100S, Dec. 2021, doi: 10.1177/15280837211057580.

[49] A. Arya, J. E. Tomlal, G. Gejo, and J. Kuruvilla, "Commingled composites of polypropylene/coir-sisal yarn: effect of chemical treatments on thermal and tensile properties," vol. 15, no. 3, pp. 169–177, 2015, doi: doi:10.1515/epoly-2014-0186.

[50] R. A. Ilyas *et al.*, "Natural Fiber-Reinforced Polylactic Acid, Polylactic Acid Blends and Their Composites for Advanced Applications," *Polymers*, vol. 14, no. 1. 2022. doi:

10.3390/polym14010202.

[51] R. M. Rasal and D. E. Hirt, "Toughness decrease of PLA-PHBHHx blend films upon surface-confined photopolymerization," *J. Biomed. Mater. Res. Part A*, vol. 88A, no. 4, pp. 1079–1086, Mar. 2009, doi: https://doi.org/10.1002/jbm.a.32009.

[52] A. A. Abir and B. Trindade, "A Comparative Study of Different Poly (Lactic Acid) Bio-Composites Produced by Mechanical Alloying and Casting for Tribological Applications," *Materials*, vol. 16, no. 4. 2023. doi: 10.3390/ma16041608.

[53] Y. Shimizu, K. Sakakibara, S. Akimoto, and Y. Tsujii, "Effective Reinforcement of Poly(methyl methacrylate) Composites with a Well-Defined Bacterial Cellulose Nanofiber Network," *ACS Sustain. Chem. Eng.*, vol. 7, no. 15, pp. 13351–13358, Aug. 2019, doi: 10.1021/acssuschemeng.9b02602.

[54] D. V Pergushov, H.-M. Buchhammer, and K. Lunkwitz, "Effect of a low-molecular-weight salt on colloidal dispersions of interpolyelectrolyte complexes," *Colloid Polym. Sci.*, vol. 277, no. 2, pp. 101–107, 1999, doi: 10.1007/PL00013742.

[55] I. Shyha, D. Huo, and J. P. Davim, "Introduction BT - Advances in Machining of Composite Materials: Conventional and Non-conventional Processes," I. Shyha and D. Huo, Eds. Cham: Springer International Publishing, 2021, pp. 1–13. doi: 10.1007/978-3-030-71438-3_1.

[56] N. van de Werken, H. Tekinalp, P. Khanbolouki, S. Ozcan, A. Williams, and M. Tehrani, "Additively manufactured carbon fiber-reinforced composites: State of the art and perspective," *Addit. Manuf.*, vol. 31, p. 100962, 2020, doi: https://doi.org/10.1016/j.addma.2019.100962.

[57] U. K. Sanivada, G. Mármol, F. P. Brito, and R. Fangueiro, "PLA Composites Reinforced with Flax and Jute Fibers—A Review of Recent Trends, Processing Parameters and Mechanical Properties," *Polymers*, vol. 12, no. 10. 2020. doi: 10.3390/polym12102373.

[58] G. Wang, D. Zhang, G. Wan, B. Li, and G. Zhao, "Glass fiber reinforced PLA composite with enhanced mechanical properties, thermal behavior, and foaming ability," *Polymer (Guildf).*, vol. 181, p. 121803, 2019, doi: https://doi.org/10.1016/j.polymer.2019.121803.

[59] A. El Magri, K. El Mabrouk, S. Vaudreuil, and M. E. Touhami, "Mechanical properties of CF-reinforced PLA parts manufactured by fused deposition modeling," *J. Thermoplast. Compos. Mater.*, vol. 34, no. 5, pp. 581–595, May 2019, doi: 10.1177/0892705719847244.

[60] M. Bayart, F. Gauvin, M. R. Foruzanmehr, S. Elkoun, and M. Robert, "Mechanical and moisture absorption characterization of PLA composites reinforced with nano-coated flax fibers," *Fibers Polym.*, vol. 18, no. 7, pp. 1288–1295, 2017, doi: 10.1007/s12221-017-7123-x.

[61] M. Bardot and M. D. Schulz, "Biodegradable Poly(Lactic Acid) Nanocomposites for Fused Deposition Modeling 3D Printing," *Nanomaterials*, vol. 10, no. 12. 2020. doi: 10.3390/nano10122567.

[62] N. D. Bikiaris *et al.*, "Recent Advances in the Investigation of Poly(lactic acid) (PLA) Nanocomposites: Incorporation of Various Nanofillers and their Properties and

Applications.," *Polymers (Basel).*, vol. 15, no. 5, Feb. 2023, doi: 10.3390/polym15051196.

[63] N. Thummarungsan, N. Paradee, D. Pattavarakorn, and A. Sirivat, "Influence of graphene on electromechanical responses of plasticized poly(lactic acid)," *Polymer (Guildf).*, vol. 138, pp. 169–179, 2018, doi: https://doi.org/10.1016/j.polymer.2018.01.069.

[64] M. Alizadeh-Osgouei, Y. Li, and C. Wen, "A comprehensive review of biodegradable synthetic polymer-ceramic composites and their manufacture for biomedical applications," *Bioact. Mater.*, vol. 4, pp. 22–36, 2019, doi: https://doi.org/10.1016/j.bioactmat.2018.11.003.

[65] X. Lacambra-Andreu, A. Maazouz, K. Lamnawar, and J.-M. Chenal, "A Review on Manufacturing Processes of Biocomposites Based on Poly(α-Esters) and Bioactive Glass Fillers for Bone Regeneration.," *Biomimetics (Basel, Switzerland)*, vol. 8, no. 1, Feb. 2023, doi: 10.3390/biomimetics8010081.

[66] M. Ly, S. Spinelli, S. Hays, and D. Zhu, "3D Printing of Ceramic Biomaterials," *Eng. Regen.*, vol. 3, no. 1, pp. 41–52, 2022, doi: https://doi.org/10.1016/j.engreg.2022.01.006.

[67] C. Maraveas, "The Sustainability of Plastic Nets in Agriculture," *Sustainability*, vol. 12, no. 9. 2020. doi: 10.3390/su12093625.

[68] N. Fijoł, A. Aguilar-Sánchez, M.-X. Ruiz-Caldas, J. Redlinger-Pohn, A. Mautner, and A. P. Mathew, "3D printed polylactic acid (PLA) filters reinforced with polysaccharide nanofibers for metal ions capture and microplastics separation from water," *Chem. Eng. J.*, vol. 457, p. 141153, 2023, doi: https://doi.org/10.1016/j.cej.2022.141153.

[69] R. T. L. Ferreira, I. C. Amatte, T. A. Dutra, and D. Bürger, "Experimental characterization and micrography of 3D printed PLA and PLA reinforced with short carbon fibers," *Compos. Part B Eng.*, vol. 124, pp. 88–100, 2017, doi: https://doi.org/10.1016/j.compositesb.2017.05.013.

[70] M. Heidari-Rarani, M. Rafiee-Afarani, and A. M. Zahedi, "Mechanical characterization of FDM 3D printing of continuous carbon fiber reinforced PLA composites," *Compos. Part B Eng.*, vol. 175, p. 107147, 2019, doi: https://doi.org/10.1016/j.compositesb.2019.107147.

[71] N. Vidakis, M. Petousis, K. Savvakis, A. Maniadi, and E. Koudoumas, "A comprehensive investigation of the mechanical behavior and the dielectrics of pure polylactic acid (PLA) and PLA with graphene (GnP) in fused deposition modeling (FDM)," *Int. J. Plast. Technol.*, vol. 23, no. 2, pp. 195–206, 2019, doi: 10.1007/s12588-019-09248-1.

[72] Y. Gao, O. T. Picot, E. Bilotti, and T. Peijs, "Influence of filler size on the properties of poly(lactic acid) (PLA)/graphene nanoplatelet (GNP) nanocomposites," *Eur. Polym. J.*, vol. 86, pp. 117–131, 2017, doi: https://doi.org/10.1016/j.eurpolymj.2016.10.045.

[73] N. Vidakis *et al.*, "Additive manufacturing of multifunctional polylactic acid (PLA)—multiwalled carbon nanotubes (MWCNTs) nanocomposites," *Nanocomposites*, vol. 7, no. 1, pp. 184–199, Jan. 2021, doi: 10.1080/20550324.2021.2000231.

[74] L. Yang *et al.*, "Effects of carbon nanotube on the thermal, mechanical, and electrical

properties of PLA/CNT printed parts in the FDM process," *Synth. Met.*, vol. 253, pp. 122–130, 2019, doi: https://doi.org/10.1016/j.synthmet.2019.05.008.

[75] T. Batakliev *et al.*, "Synergistic Effect of Graphene Nanoplatelets and Multiwall Carbon Nanotubes Incorporated in PLA Matrix: Nanoindentation of Composites with Improved Mechanical Properties," *J. Mater. Eng. Perform.*, vol. 30, no. 5, pp. 3822–3830, 2021, doi: 10.1007/s11665-021-05679-3.

[76] E. P. Mohammed Basheer and K. Marimuthu, "Carbon fibre-graphene composite polylactic acid (PLA) material for COVID shield frame," *Materwiss. Werksttech.*, vol. 53, no. 1, pp. 119–127, Jan. 2022, doi: https://doi.org/10.1002/mawe.202100154.

[77] T. Batakliev, "Tribological investigation of pla-based nanocomposites by scratch and wear experiments," *J. Theor. Appl. Mech.*, vol. 50, no. 2, pp. 105–113, 2020, doi: 10.7546/jtam.50.20.02.01.

[78] J. Bustillos, D. Montero, P. Nautiyal, A. Loganathan, B. Boesl, and A. Agarwal, "Integration of graphene in poly(lactic) acid by 3D printing to develop creep and wear-resistant hierarchical nanocomposites," *Polym. Compos.*, vol. 39, no. 11, pp. 3877–3888, Nov. 2018, doi: https://doi.org/10.1002/pc.24422.

[79] B. Suresha, V. Hanamasagar, and A. Anand, "Processing and tribological behaviour of carbon fiber reinforced polylactic acid composites," *IOP Conf. Ser. Mater. Sci. Eng.*, vol. 1272, no. 1, p. 12022, 2022, doi: 10.1088/1757-899X/1272/1/012022.

[80] L. Vaiani *et al.*, "Ceramic Materials for Biomedical Applications: An Overview on Properties and Fabrication Processes.," *J. Funct. Biomater.*, vol. 14, no. 3, Mar. 2023, doi: 10.3390/jfb14030146.

[81] D. L. P. Macuvele *et al.*, "UHMWPE/HA biocomposite compatibilized by organophilic montmorillonite: An evaluation of the mechanical-tribological properties and its hemocompatibility and performance in simulated blood fluid," *Mater. Sci. Eng. C*, vol. 100, pp. 411–423, 2019, doi: https://doi.org/10.1016/j.msec.2019.02.102.

[82] L. Xiong, D. Xiong, Y. Yang, and J. Jin, "Friction, wear, and tensile properties of vacuum hot pressing crosslinked UHMWPE/nano-HAP composites," *J. Biomed. Mater. Res. Part B Appl. Biomater.*, vol. 98B, no. 1, pp. 127–138, Jul. 2011, doi: https://doi.org/10.1002/jbm.b.31842.

[83] S. A. Mirsalehi, A. Khavandi, S. Mirdamadi, M. R. Naimi-Jamal, and S. M. Kalantari, "Nanomechanical and tribological behavior of hydroxyapatite reinforced ultrahigh molecular weight polyethylene nanocomposites for biomedical applications," *J. Appl. Polym. Sci.*, vol. 132, no. 23, Jun. 2015, doi: https://doi.org/10.1002/app.42052.

[84] A. V Maksimkin, S. D. Kaloshkin, V. V Tcherdyntsev, F. S. Senatov, and V. D. Danilov, "Structure and properties of ultra-high molecular weight polyethylene filled with disperse hydroxyapatite," *Inorg. Mater. Appl. Res.*, vol. 3, no. 4, pp. 288–295, 2012, doi: 10.1134/S2075113312040132.

[85] X. Kang, W. Zhang, and C. Yang, "Mechanical properties study of micro- and nano-hydroxyapatite reinforced ultrahigh molecular weight polyethylene composites," *J. Appl. Polym. Sci.*, vol. 133, no. 3, Jan. 2016, doi: https://doi.org/10.1002/app.42869.

[86] M. L. Tan, P. F. M. Choong, and C. R. Dass, "Recent developments in liposomes, microparticles and nanoparticles for protein and peptide drug delivery.," *Peptides*, vol. 31, no. 1, pp. 184–193, Jan. 2010, doi: 10.1016/j.peptides.2009.10.002.

[87] M.-A. Valantin *et al.*, "Polylactic acid implants (New-Fill) to correct facial lipoatrophy in HIV-infected patients: results of the open-label study VEGA.," *AIDS*, vol. 17, no. 17, pp. 2471–2477, Nov. 2003, doi: 10.1097/00002030-200311210-00009.

[88] D. Hayman, C. Bergerson, S. Miller, M. Moreno, and J. E. Moore, "The Effect of Static and Dynamic Loading on Degradation of PLLA Stent Fibers," *J. Biomech. Eng.*, vol. 136, no. 8, Jun. 2014, doi: 10.1115/1.4027614.

[89] C. Nakafuku and S. Takehisa, "Glass transition and mechanical properties of PLLA and PDLLA-PGA copolymer blends," *J. Appl. Polym. Sci.*, vol. 93, no. 5, pp. 2164–2173, Sep. 2004, doi: https://doi.org/10.1002/app.20687.

[90] J. S. Bergström and D. Hayman, "An Overview of Mechanical Properties and Material Modeling of Polylactide (PLA) for Medical Applications," *Ann. Biomed. Eng.*, vol. 44, no. 2, pp. 330–340, 2016, doi: 10.1007/s10439-015-1455-8.

[91] T. Maharana, B. Mohanty, and Y. S. Negi, "Melt–solid polycondensation of lactic acid and its biodegradability," *Prog. Polym. Sci.*, vol. 34, no. 1, pp. 99–124, 2009, doi: https://doi.org/10.1016/j.progpolymsci.2008.10.001.

[92] R. Langer, "Drug delivery and targeting," *Nature*, vol. 392, no. 6679 Suppl, pp. 5–10, 1998, [Online]. Available: http://europepmc.org/abstract/MED/9579855

[93] J. E. Bergsma, W. C. de Bruijn, F. R. Rozema, R. R. Bos, and G. Boering, "Late degradation tissue response to poly(L-lactide) bone plates and screws.," *Biomaterials*, vol. 16, no. 1, pp. 25–31, Jan. 1995, doi: 10.1016/0142-9612(95)91092-d.

[94] S. W. Shalaby and A. L. Allen, "Biomedical polymers : designed-to-degrade systems," 1994.

[95] L. T. D. Amar K. Mohanty, Manjusri Misra, *Natural Fibers, Biopolymers, and Biocomposites*, 1st ed. CRC Press, 2005. doi: 10.1201/9780203508206.

[96] S. Jacobsen and H. G. Fritz, "Plasticizing polylactide—the effect of different plasticizers on the mechanical properties," *Polym. Eng. Sci.*, vol. 39, no. 7, pp. 1303–1310, Jul. 1999, doi: https://doi.org/10.1002/pen.11517.

[97] T. M. Joseph *et al.*, "3D printing of polylactic acid: recent advances and opportunities," *Int. J. Adv. Manuf. Technol.*, vol. 125, no. 3, pp. 1015–1035, 2023, doi: 10.1007/s00170-022-10795-y.

[98] B. C. Gross, J. L. Erkal, S. Y. Lockwood, C. Chen, and D. M. Spence, "Evaluation of 3D printing and its potential impact on biotechnology and the chemical sciences.," *Anal. Chem.*, vol. 86, no. 7, pp. 3240–3253, Apr. 2014, doi: 10.1021/ac403397r.

[99] H. N. Chia and B. M. Wu, "Recent advances in 3D printing of biomaterials," *J. Biol. Eng.*, vol. 9, no. 1, p. 4, 2015, doi: 10.1186/s13036-015-0001-4.

[100] A. Al Abir, D. Chakrabarti, and B. Trindade, "Fused Filament Fabricated Poly(lactic acid) Parts Reinforced with Short Carbon Fiber and Graphene Nanoparticles with Improved Tribological Properties," *Polymers*, vol. 15, no. 11. 2023. doi: 10.3390/polym15112451.

[101] A. V. Girão, G. Caputo, and M. C. Ferro, "Chapter 6 - Application of Scanning Electron Microscopy–Energy Dispersive X-Ray Spectroscopy (SEM-EDS)," in *Characterization and Analysis of Microplastics*, vol. 75, T. A. P. Rocha-Santos and A. C. B. T.-C. A. C. Duarte, Eds. Elsevier, 2017, pp. 153–168. doi: https://doi.org/10.1016/bs.coac.2016.10.002.

[102] A. Rashidi, T. Olfatbakhsh, B. Crawford, and A. S. Milani, "A Review of Current Challenges and Case Study toward Optimizing Micro-Computed X-Ray Tomography of Carbon Fabric Composites.," *Mater. (Basel, Switzerland)*, vol. 13, no. 16, Aug. 2020, doi: 10.3390/ma13163606.

[103] R. Allemang, J. De Clerck, C. Niezrecki, and A. Wicks, "Preface," *Conf. Proc. Soc. Exp. Mech. Ser.*, vol. 45, no. 7, pp. 577–617, 2014.

[104] J. Thomas and P. Leroux, *Composite Material Analysis using 3D Profilometry*. 2020.

[105] P. H. Bucksbaum, M. R. Ware, A. Natan, J. P. Cryan, and J. M. Glownia, "Characterizing Multiphoton Excitation Using Time-Resolved X-ray Scattering," *Phys. Rev. X*, vol. 10, no. 1, p. 11065, Mar. 2020, doi: 10.1103/PhysRevX.10.011065.

[106] M. H. Chiu and E. J. Prenner, "Differential scanning calorimetry: An invaluable tool for a detailed thermodynamic characterization of macromolecules and their interactions.," *J. Pharm. Bioallied Sci.*, vol. 3, no. 1, pp. 39–59, Jan. 2011, doi: 10.4103/0975-7406.76463.

[107] J. E. Campbell and T. W. Clyne, Eds., "Hardness Testing," in *Testing of the Plastic Deformation of Metals*, Cambridge: Cambridge University Press, 2021, pp. 123–147. doi: DOI: 10.1017/9781108943369.008.

[108] "Shore A Versus Shore D: The Important Differences You Need to Know," *Apple Rubber*, 2021. http://www.applerubber.com/blog/shore-a-versus-shore-d-the-important-differences-you-need-to-know/ (accessed Jun. 21, 2023).

[109] A. Standard, "ASTM E 1876-01: standard test method for dynamic young's modulus, shear modulus, and poisson's ratio by impulse excitation of vibration," *Annu. B. ASTM Stand. ASTM, West Conshohocken, PA*, 2015.

[110] J. Jozwik, K. Dziedzic, M. Barszcz, and M. Pashechko, "Analysis and Comparative Assessment of Basic Tribological Properties of Selected Polymer Composites.," *Mater. (Basel, Switzerland)*, vol. 13, no. 1, Dec. 2019, doi: 10.3390/ma13010075.

[111] C. Birleanu *et al.*, "Tribo-Mechanical Investigation of Glass Fiber Reinforced Polymer Composites under Dry Conditions," *Polymers*, vol. 15, no. 12. 2023. doi: 10.3390/polym15122733.

[112] S. Kucharski and Z. Mróz, "Identification of wear process parameters in reciprocating ball-

on-disc tests," *Tribol. Int.*, vol. 44, no. 2, pp. 154–164, 2011, doi: https://doi.org/10.1016/j.triboint.2010.10.010.

[113] S. Hara, S. Watanabe, K. Takahashi, S. Shimizu, and H. Ikake, "Preparation of Crystallites for Oriented Poly(Lactic Acid) Films Using a Casting Method under a Magnetic Field," *Polymers*, vol. 10, no. 10. 2018. doi: 10.3390/polym10101083.

[114] V. Kosma *et al.*, "Fibrous hydroxyapatite–carbon nanotube composites by chemical vapor deposition: In situ fabrication, structural and morphological characterization," *Mater. Sci. Eng. B*, Sep. 2012.

[115] M. A. Ruz-Cruz, P. J. Herrera-Franco, E. A. Flores-Johnson, M. V Moreno-Chulim, L. M. Galera-Manzano, and A. Valadez-González, "Thermal and mechanical properties of PLA-based multiscale cellulosic biocomposites," *J. Mater. Res. Technol.*, vol. 18, pp. 485–495, 2022, doi: https://doi.org/10.1016/j.jmrt.2022.02.072.

[116] M. Vinyas, S. J. Athul, D. Harursampath, and T. Nguyen Thoi, "Experimental evaluation of the mechanical and thermal properties of 3D printed PLA and its composites," *Mater. Res. Express*, vol. 6, no. 11, p. 115301, 2019, doi: 10.1088/2053-1591/ab43ab.

[117] A. Sorrentino, F. De Santis, and G. Titomanlio, "Polymer Crystallization Under High Cooling Rate and Pressure: A Step Towards Polymer Processing Conditions BT - Progress in Understanding of Polymer Crystallization," G. Reiter and G. R. Strobl, Eds. Berlin, Heidelberg: Springer Berlin Heidelberg, 2007, pp. 329–344. doi: 10.1007/3-540-47307-6_16.

[118] J. M. Ferri, I. Gisbert, D. García-Sanoguera, M. J. Reig, and R. Balart, "The effect of beta-tricalcium phosphate on mechanical and thermal performances of poly(lactic acid)," *J. Compos. Mater.*, vol. 50, no. 30, pp. 4189–4198, Mar. 2016, doi: 10.1177/0021998316636205.

[119] T. Standau, C. Zhao, S. Murillo Castellón, C. Bonten, and V. Altstädt, "Chemical Modification and Foam Processing of Polylactide (PLA)," *Polymers*, vol. 11, no. 2. 2019. doi: 10.3390/polym11020306.

[120] S. A. Tronvoll, N. P. Vedvik, C. W. Elverum, and T. Welo, "A new method for assessing anisotropy in fused deposition modeled parts using computed tomography data," *Int. J. Adv. Manuf. Technol.*, vol. 105, no. 1, pp. 47–65, 2019, doi: 10.1007/s00170-019-04081-7.

[121] S. Liu, Y. Zheng, R. Liu, and C. Tian, "Preparation and characterization of a novel polylactic acid/hydroxyapatite composite scaffold with biomimetic micro-nanofibrous porous structure," *J. Mater. Sci. Mater. Med.*, vol. 31, no. 8, p. 74, 2020, doi: 10.1007/s10856-020-06415-4.

[122] L.-S. Zhao and Y.-H. Cai, "Studies of Poly(L-lactic acid)/Hydroxyapatite Composites Through DSC and XRD," *IOP Conf. Ser. Mater. Sci. Eng.*, vol. 439, no. 4, p. 42049, 2018, doi: 10.1088/1757-899X/439/4/042049.

[123] Y. Chen, Y. Qi, Z. Tai, X. Yan, F. Zhu, and Q. Xue, "Preparation, mechanical properties and biocompatibility of graphene oxide/ultrahigh molecular weight polyethylene composites," *Eur. Polym. J.*, vol. 48, no. 6, pp. 1026–1033, 2012, doi:

https://doi.org/10.1016/j.eurpolymj.2012.03.011.

[124] N. W. Khun, B. C. R. Troconis, and G. S. Frankel, "Effects of carbon nanotube content on adhesion strength and wear and corrosion resistance of epoxy composite coatings on AA2024-T3," *Prog. Org. Coatings*, vol. 77, no. 1, pp. 72–80, 2014, doi: https://doi.org/10.1016/j.porgcoat.2013.08.003.

[125] M. Terrones, "Science and Technology of the Twenty-First Century: Synthesis, Properties, and Applications of Carbon Nanotubes," *Annu. Rev. Mater. Res.*, vol. 33, no. 1, pp. 419–501, Aug. 2003, doi: 10.1146/annurev.matsci.33.012802.100255.

[126] D. L. P. Macuvele *et al.*, "UHMWPE/HA biocomposite compatibilized by organophilic montmorillonite: An evaluation of the mechanical-tribological properties and its hemocompatibility and performance in simulated blood fluid," *Mater. Sci. Eng. C*, vol. 100, no. June 2018, pp. 411–423, 2019, doi: 10.1016/j.msec.2019.02.102.

[127] J. Fernandes, A. M. Deus, L. Reis, M. F. Vaz, and M. Leite, "Study of the influence of 3D printing parameters on the mechanical properties of PLA," *Proc. Int. Conf. Prog. Addit. Manuf.*, vol. 2018-May, pp. 547–552, 2018, doi: 10.25341/D4988C.

[128] J. Kang, J. Zheng, Y. Hui, and D. Li, "Mechanical Properties of 3D-Printed PEEK/HA Composite Filaments," *Polymers*, vol. 14, no. 20. 2022. doi: 10.3390/polym14204293.

[129] Y.-H. Zhao, Y.-F. Zhang, S.-L. Bai, and X.-W. Yuan, "Carbon fibre/graphene foam/polymer composites with enhanced mechanical and thermal properties," *Compos. Part B Eng.*, vol. 94, pp. 102–108, 2016, doi: https://doi.org/10.1016/j.compositesb.2016.03.056.

[130] Y. Abderrafai *et al.*, "Additive manufacturing of short carbon fiber-reinforced polyamide composites by fused filament fabrication: Formulation, manufacturing and characterization," *Mater. Des.*, vol. 214, p. 110358, 2022, doi: https://doi.org/10.1016/j.matdes.2021.110358.

[131] C. Ozkan, N. Gamze Karsli, A. Aytac, and V. Deniz, "Short carbon fiber reinforced polycarbonate composites: Effects of different sizing materials," *Compos. Part B Eng.*, vol. 62, pp. 230–235, 2014, doi: https://doi.org/10.1016/j.compositesb.2014.03.002.

[132] M. M. Hanon, A. Ghaly, L. Zsidai, and S. Klébert, "Tribological characteristics of digital light processing (DLP) 3D printed graphene/resin composite: Influence of graphene presence and process settings," *Mater. Des.*, vol. 218, p. 110718, 2022, doi: https://doi.org/10.1016/j.matdes.2022.110718.

[133] A. Torres Marques, S. Esteves, J. P. Pereira, and L. M. Oliveira, *Additive Manufacturing Hybrid Processes for Composites Systems*, vol. 129. 2020. [Online]. Available: http://link.springer.com/10.1007/978-3-030-44522-5

[134] S. Jia, D. Yu, Y. Zhu, Z. Wang, L. Chen, and L. Fu, "Morphology, Crystallization and Thermal Behaviors of PLA-Based Composites: Wonderful Effects of Hybrid GO/PEG via Dynamic Impregnating.," *Polymers (Basel).*, vol. 9, no. 10, Oct. 2017, doi: 10.3390/polym9100528.

[135] R. C. Nonato, L. H. I. Mei, B. C. Bonse, E. F. Chinaglia, and A. R. Morales, "Nanocomposites of PLA containing ZnO nanofibers made by solvent cast 3D printing: Production and characterization," *Eur. Polym. J.*, vol. 114, pp. 271–278, 2019, doi: https://doi.org/10.1016/j.eurpolymj.2019.02.026.

[136] F. J. Carrión, J. Sanes, and M.-D. Bermúdez, "Influence of ZnO nanoparticle filler on the properties and wear resistance of polycarbonate," *Wear*, vol. 262, no. 11, pp. 1504–1510, 2007, doi: https://doi.org/10.1016/j.wear.2007.01.016.

[137] D. Berman, A. Erdemir, and A. V Sumant, "Graphene: a new emerging lubricant," *Mater. Today*, vol. 17, no. 1, pp. 31–42, 2014, doi: https://doi.org/10.1016/j.mattod.2013.12.003.

[138] G. Mittal, V. Dhand, K. Y. Rhee, S.-J. Park, and W. R. Lee, "A review on carbon nanotubes and graphene as fillers in reinforced polymer nanocomposites," *J. Ind. Eng. Chem.*, vol. 21, pp. 11–25, 2015, doi: https://doi.org/10.1016/j.jiec.2014.03.022.

[139] K. Friedrich, "Polymer composites for tribological applications," *Adv. Ind. Eng. Polym. Res.*, vol. 1, no. 1, pp. 3–39, 2018, doi: https://doi.org/10.1016/j.aiepr.2018.05.001.

[140] V. Rodriguez, J. Sukumaran, A. K. Schlarb, and P. De Baets, "Reciprocating sliding wear behaviour of PEEK-based hybrid composites," *Wear*, vol. 362–363, pp. 161–169, 2016, doi: https://doi.org/10.1016/j.wear.2016.05.024.

[141] X. Shi, Y. Bin, D. Hou, and M. Matsuo, "Surface Characterization for Ultrahigh Molecular Weight Polyethylene/Hydroxyapatite Gradient Composites Prepared by the Gelation/Crystallization Method," *ACS Appl. Mater. Interfaces*, vol. 5, no. 5, pp. 1768–1780, Mar. 2013, doi: 10.1021/am3030504.

[142] C. J. Schwartz, S. Bahadur, and S. K. Mallapragada, "Effect of crosslinking and Pt–Zr quasicrystal fillers on the mechanical properties and wear resistance of UHMWPE for use in artificial joints," *Wear*, vol. 263, no. 7, pp. 1072–1080, 2007, doi: https://doi.org/10.1016/j.wear.2006.10.023.

[143] J. K. Lancaster, "Abrasive wear of polymers," *Wear*, vol. 14, no. 4, pp. 223–239, 1969, doi: https://doi.org/10.1016/0043-1648(69)90047-7.